arXiv:hep-ph/0306165v2 14 Jan 2004

Axial-vector Form Factors for $K_{l2\gamma}$ and $\pi_{l2\gamma}$ at $O(p^6)$ in Chiral Perturbation Theory

C.Q. Geng[1,2], I-Lin Ho[1], and T.H. Wu[1*]

[1]Department of Physics, National Tsing Hua University
Hsinchu, Taiwan
[2] Theory Group, TRIUMF
Vancouver, B.C. V3T 2A3, Canada

February 1, 2008

Abstract

We present two-loop calculations on the axial-vector form factors F_A of semileptonic radiative kaon and pion decays in chiral perturbation theory. The relevant dimension-6 terms of the lagrangian are evaluated from the resonance contribution and the results of the irreducible two-loop graphs of the sunset topology are given in detail. We also explicitly show that the divergent parts in F_A are cancelled exactly as required.

1 Introduction

Chiral perturbation theory (ChPT) [1, 2] has established itself as a powerful effective theory of low energy interactions. While it works for the strong interaction, it also includes the electroweak one whose dynamics can be completely fixed by introducing the corresponding gauge bosons through the usual covariant derivative. Since the external momenta and quark masses are the expansion parameters for the generating function in ChPT [3, 4, 5], they need to be small compared to the physical scale of the chiral symmetry breaking, i.e. about 1 GeV. Therefore, one expects that the semileptonic radiative kaon (pion) decays of $K^+ \to l^+\nu_l\gamma$ ($\pi^+ \to l^+\nu_l\gamma$) can be well described in ChPT [6, 7]. It is known that these radiative decays [8, 9, 10, 11] could provide us with information on new physics [12, 13] by searching for the lepton polarization effects, which depend on the vector and axial-vector form factors $F_{V,A}$ of the structure dependent parts.

In this paper we deal mainly with the $SU(3) \otimes SU(3)$ chiral symmetry. We will present two-loop calculations on the axial-vector form factors in $K^+ \to l^+\nu_l\gamma$ ($K_{l2\gamma}$) and $\pi^+ \to l^+\nu_l\gamma$ ($\pi_{l2\gamma}$) by virtue of the recent progresses in the p^6-Lagrangian [14, 15, 16] and the massive two-loop integrals [17, 18]. Some remarks related to the form factors in $K_{l2\gamma}$ and $\pi_{l2\gamma}$ follow:

---

[*] Deceased

- The usual one-loop ChPT for the timelike form factor does not satisfy the unitarity or the final-state theorem and makes poor approximations [19, 20, 21]. Substantial corrections are expected at a higher order, especially at the two-loop level.

- The form factors in the decays receive the first non-vanishing contributions at $O(p^4)$ but the first sizable ones, as well as the estimates of the accuracy, arise at $O(p^6)$.

- The question of convergence in ChPT needs to be clearly addressed [22].

- In ChPT, the $O(p^6)$ contributions to the vector form factors F_V in the decays have been studied in Ref. [23], but those to the axial-vector ones F_A have been done only for $\pi \to l\nu_l\gamma$ based on the $SU(2) \times SU(2)$ symmetry [24].

In this paper, by using the relevant dimension-6 terms of the lagrangian [18, 20] from the resonance contribution [23, 24, 25], we perform a detailed calculation for the irreducible two-loop graphs of the sunset topology [21], which give the dominant contributions to F_A in both π and K decays at $O(p^6)$. For completeness, we will also evaluate F_V and compare our results with those in Ref. [23].

The paper is organized as follows. In Sec. 2, we give the matrix elements for the decays. We review the lagrangians of ChPT to $O(p^6)$ in Sec. 3. In Sec. 4, we display the two-loop calculations for both vector and axial-vector form factors with the detailed formulas placed in Appendices A, B and C. In Sec. 5, we show the analytical results. We present our numerical values and conclusions in Sec. 6.

2 The matrix elements

We consider the decay of $P(p) \to l^+(l')\nu_l(s')\gamma(k)$ with $P = K^+$ or π^+, where γ is a real photon with $k^2 = 0$. The matrix element M for the decay [6, 26, 27] can be written as

$$M_{P\to l^+\nu_l\gamma} = -i\frac{eG_F}{\sqrt{2}}\theta_P M_{\mu\nu}(p,k)\epsilon^{\mu *}(k)\overline{u}(s')\gamma^\nu(1-\gamma_5)v(l')\,, \tag{1}$$

where ϵ^μ is the photon polarization and $\theta_{K^+(\pi^+)} = \cos\theta\,(\sin\theta)$ with θ being the Cabibbo angle. In Eq. (1), the hadronic part of the quantity $M_{\mu\nu}$ is given by

$$M_{\mu\nu}(p,k) \;=\; \int d^4x e^{iq\cdot x}\left\langle 0\left|T(J^{em}_\mu(x)J^{wk}_\nu(0))\right|P(p)\right\rangle\,, \tag{2}$$

which has the general structure

$$\begin{aligned} M_{\mu\nu}(p,k) \;=\; & -\sqrt{2}F_P\frac{(p-k)_\nu}{(p-k)^2-M_P^2}\left\langle P(p-k)\left|J^{em}_\mu\right|P(p)\right\rangle + \sqrt{2}F_P g_{\mu\nu} \\ & -F_A[(p-k)_\mu k_\nu - g_{\mu\nu}k\cdot(p-k)] - r_A(k_\mu k_\nu - g_{\mu\nu}k^2) \\ & +iF_V\varepsilon_{\mu\nu\alpha\beta}k^\alpha p^\beta \end{aligned} \tag{3}$$

where the first line represents the Born diagram, in which the photon couples to hadrons through the known $KK\gamma$ $(\pi\pi\gamma)$ coupling, with F_P being the P meson decay constant, and the subsequent lines correspond to axial-vector and vector portions of the weak currents with $F_{V(A)}$ being the vector (axial-vector) form factor. In Eq. (3), r_A is non-zero only for those processes with virtual photons, such as $P^- \to l^+ l^+ l^- \overline{\nu}_l$. In terms of the form factors F_A and F_V, we can write the vector and axial-vector parts in Eqs. (1) and (3) as

$$M_V(P \quad \to \quad l^+ \nu_l \gamma) = \frac{eG_F\theta_P}{\sqrt{2}} F_V \varepsilon_{\mu\nu\alpha\beta} \epsilon^{\mu *} l^\nu k^\alpha p^\beta \,, \tag{4}$$

$$M_A(P \quad \to \quad l^+ \nu_l \gamma) = i\frac{eG_F\theta_P}{\sqrt{2}} F_A l^\nu [k_\nu (p\cdot\epsilon) - g_{\mu\nu}(p\cdot k)\epsilon^{\mu *}] \,, \tag{5}$$

respectively, where

$$l^\nu = \overline{u}(s')\gamma^\nu (1-\gamma_5) v(l') \,. \tag{6}$$

Both F_A and F_V are real functions for $q^2 \equiv (p-k)^2$ below the physical threshold, which is the region of interest here, based on time-reversal invariance, and they are analytic functions of q^2 with cuts on the positive real axis. One of the reasons to perform the present calculation is that the q^2 dependence of the form factors starts at $O(p^6)$.

3 The Lagrangians of chiral perturbation theory

In the usual formulation of ChPT [1, 2, 28] with the chiral symmetry $SU(3)_L \times SU(3)_R$, the pseudoscalar fields are collected in a unitary 3×3 matrix

$$U(x) = exp\left(i\frac{\Phi(x)}{F}\right) \,, \tag{7}$$

where F absorbs the dimensional dependence of the fields and, in the chiral limit, is equal to the pion decay constant, $F_\pi = 92.4$ MeV. The Φ is given by the 3×3 matrix

$$\Phi = \lambda_a \varphi_a = \left(\begin{array}{ccc} \pi^0 + \frac{\eta}{\sqrt{3}} & \sqrt{2}\pi^+ & \sqrt{2}K^+ \\ \sqrt{2}\pi^- & -\pi^0 + \frac{\eta}{\sqrt{3}} & \sqrt{2}K^0 \\ \sqrt{2}K^- & \sqrt{2}\overline{K}^0 & \frac{-2\eta}{\sqrt{3}} \end{array} ,\right) \tag{8}$$

where λ_a $(a = 1, 2, \cdots, 8)$ are the Gell-Mann matrices.

An explicit breaking of the chiral symmetry is introduced via the mass matrix

$$\chi = \left(\begin{array}{ccc} m_\pi^2 & 0 & 0 \\ 0 & m_\pi^2 & 0 \\ 0 & 0 & 2m_K^2 - m_\pi^2 \end{array} ,\right) \tag{9}$$

where $m_{\pi(K)}$ is the unrenormalized π (K) mass. We note that the mass of η to this order is given by the Gell-Mann-Okubo relation

$$m_\eta^2 = \frac{4}{3}m_K^2 - \frac{1}{3}m_\pi^2 \,. \tag{10}$$

The mass term in Eq. (9) is related to the quark masses by $\chi = const \cdot diag(m_u, m_d, m_s)$ with $m_u = m_d$. To calculate the form factors, we have to include the interaction with external boson fields. As previously stated, the electroweak gauge fields A_μ and W_μ are introduced via the covariant derivative

$$\begin{aligned} D_\mu U &= \partial_\mu U + iU\ell_\mu - ir_\mu U\,, \\ \ell_\mu &= eA_\mu Q - \frac{g}{\sqrt{2}}\begin{pmatrix} 0 & \cos\theta W_\mu^+ & \sin\theta W_\mu^+ \\ \cos\theta W_\mu^- & 0 & 0 \\ \sin\theta W_\mu^- & 0 & 0 \end{pmatrix}, \\ r_\mu &= eA_\mu Q\,, \end{aligned} \tag{11}$$

where Q is the quark charge matrix in units of $e = g\sin\theta_W$, with θ_W standing for the Weinberg angles and $G_F/\sqrt{2} = g^2/(8M_W^2)$. The final lepton pair (for clearity we will always refer to $l^+\nu_l$ coming from W^+) appears in the leptonic current when substituting

$$W_\mu \to \frac{g}{2\sqrt{2}M_W^2} l_\mu = \frac{g}{2\sqrt{2}M_W^2}\overline{u}(s)\gamma_\mu(1-\gamma_5)v(l)\,. \tag{12}$$

The Lagrangians of ChPT contain both normal (or non-anomalous) and anomalous parts. Since the form factor F_V is related by an isospin rotation to the amplitude for $\pi^0 \to \gamma\gamma$, it can be absolutely predicted from the axial anomaly. For this reason, we must also include the effect of the axial anomaly. At the two lowest orders, the full non-anomalous Lagrangian is given by [1, 2]

$$\mathcal{L}_n^{(2)} = \frac{F^2}{4}Tr(D_\mu U D^\mu U^\dagger) + \frac{F^2}{4}Tr(\chi U^\dagger + U\chi^\dagger)\,, \tag{13}$$

$$\begin{aligned} \mathcal{L}_n^{(4)} = {}& L_1\left[Tr(D_\mu U D^\mu U^\dagger)\right]^2 + L_2 Tr(D_\mu U D_\nu U^\dagger)Tr(D^\mu U D^\nu U^\dagger) \\ &+L_3 Tr(D_\mu U D^\mu U^\dagger D_\nu U D^\nu U^\dagger) \\ &+L_4 Tr(D_\mu U D^\mu U^\dagger)Tr(\chi U^\dagger + U\chi^\dagger) \\ &+L_5 Tr(D_\mu U D^\mu U^\dagger(\chi U^\dagger + U\chi^\dagger)) + L_6\left[Tr(\chi U^\dagger + U\chi^\dagger)\right]^2 \\ &+L_7\left[Tr(\chi^\dagger U - U^\dagger\chi)\right]^2 + L_8 Tr(\chi U^\dagger \chi U^\dagger + U\chi^\dagger U\chi^\dagger) \\ &+iL_9 Tr(L_{\mu\nu}D^\mu U D^\nu U^\dagger + R_{\mu\nu}D^\mu U^\dagger D^\nu U) + L_{10}Tr(L_{\mu\nu}UR_{\mu\nu}U^\dagger)\,, \end{aligned} \tag{14}$$

where $L_{\mu\nu}$ and $R_{\mu\nu}$ are the field-strength tensors of external sources, defined by

$$\begin{aligned} L_{\mu\nu} &= \partial_\mu \ell_\nu - \partial_\nu \ell_\mu - i\left[\ell_\mu, \ell_\nu\right]\,, \\ R_{\mu\nu} &= \partial_\mu r_\nu - \partial_\nu r_\mu - i\left[r_\mu, r_\nu\right]\,, \end{aligned} \tag{15}$$

and $\{L_i\}$ are unrenormalized coupling constants. At $O(p^6)$, the non-anomalous Chiral Lagrangian contains 90 independent terms plus four contact terms for $SU(3)$ [18]. The terms relevant to $K_{l2\gamma}$ ($\pi_{l2\gamma}$) decays are found to be

$$\begin{aligned} \mathcal{L}_n^{(6)} = {}& y_{17}\langle\chi_+ h_{\mu\nu}h^{\mu\nu}\rangle + y_{18}\langle\chi_+\rangle\langle h_{\mu\nu}h^{\mu\nu}\rangle + y_{81}\langle\chi_+ f_{+\mu\nu}f_+^{\mu\nu}\rangle \\ &+y_{82}\langle\chi_+\rangle\langle f_{+\mu\nu}f_+^{\mu\nu}\rangle + iy_{83}\langle f_{+\mu\nu}\{\chi_+, u^\mu u^\nu\}\rangle + iy_{84}\langle\chi_+\rangle\langle f_{+\mu\nu}u^\mu u^\nu\rangle \\ &+iy_{85}\langle f_{+\mu\nu}u^\mu\chi_+ u^\nu\rangle + iy_{100}\left\langle f_{+\mu\nu}\left[f_-^{\nu\rho}, h_\rho^\mu\right]\right\rangle + y_{102}\langle\chi_+ f_{-\mu\nu}f_-^{\mu\nu}\rangle \\ &+y_{103}\langle\chi_+\rangle\langle f_{-\mu\nu}f_-^{\mu\nu}\rangle + y_{104}\langle f_{+\mu\nu}\left[f_-^{\mu\nu}, \chi_-\right]\rangle + y_{109}\langle\nabla_\rho f_{-\mu\nu}\nabla^\rho f_-^{\mu\nu}\rangle \\ &+iy_{110}\langle\nabla_\rho f_{+\mu\nu}\left[h^{\mu\rho}, u^\nu\right]\rangle + \ldots\,, \end{aligned} \tag{16}$$

where

$$\begin{aligned}
u_\mu &= i\left\{U^\dagger(\partial_\mu - ir_\mu)U - U(\partial_\mu - i\ell_\mu)U^\dagger\right\}\,, \\
\chi_\pm &= U^\dagger \chi U^\dagger + U\chi^\dagger U\,, \\
f_\pm^{\mu\nu} &= UL^{\mu\nu}U^\dagger \pm U^\dagger R^{\mu\nu}U\,, \\
h_{\mu\nu} &= \nabla_\mu u_\nu + \nabla_\nu u_\mu\,, \\
\chi_{\pm\mu} &= U^\dagger D_\mu \chi U^\dagger \pm U D_\mu \chi^\dagger U = \nabla_\mu \chi_\pm - \frac{i}{2}\left\{\chi_\mp, u_\mu\right\}\,.
\end{aligned} \tag{17}$$

The covariant derivative $\nabla_\mu X = \partial_\mu X + [\Gamma_\mu, X]$ is defined in terms of the chiral condition

$$\Gamma_\mu = \frac{1}{2}\left\{U^\dagger(\partial_\mu - ir_\mu)U - U(\partial_\mu - i\ell_\mu)U^\dagger\right\}\,. \tag{18}$$

The anomalous part begins at $O(p^4)$ with the Wess-Zumino (WZ) term $\mathcal{L}_{WZ}$ [29] containing pieces with zero, one and two gauge boson fields. The terms with one and two gauge bosons as well as the anomalous p^6-Lagiangian [20, 29] are given by

$$\mathcal{L}_{WZ,1}^{(4)} = -\frac{1}{16\pi^2}\varepsilon^{\mu\nu\alpha\beta} tr(U\partial_\mu U^\dagger \partial_\nu U \partial_\alpha U^\dagger \ell_\beta - U^\dagger \partial_\mu U \partial_\nu U^\dagger \partial_\alpha U r_\beta)\,, \tag{19}$$

$$\begin{aligned}
\mathcal{L}_{WZ,2}^{(4)} &= -\frac{i}{16\pi^2}\varepsilon^{\mu\nu\alpha\beta} tr(\partial_\mu U^\dagger \partial_\nu \ell_\alpha U r_\beta - \partial_\mu U \partial_\nu r_\alpha U^\dagger \ell_\beta) \\
&\quad + U\partial_\mu U^\dagger(\ell_\nu \partial_\alpha \ell_\beta + \partial_\nu \ell_\alpha \ell_\beta)\,,
\end{aligned} \tag{20}$$

$$\begin{aligned}
\mathcal{L}_a^{(6)} &= iC_7 \varepsilon^{\mu\nu\alpha\beta}\left\langle \chi_- f_{+\mu\nu} f_{+\alpha\beta}\right\rangle + iC_{11}\varepsilon^{\mu\nu\alpha\beta}\left\langle \chi_-[f_{+\mu\nu}, f_{-\alpha\beta}]\right\rangle \\
&\quad + C_{22}\varepsilon^{\mu\nu\alpha\beta}\left\langle u_\mu\{\nabla_\gamma f_{+\gamma\nu}, f_{+\alpha\beta}\}\right\rangle + \cdots\,.
\end{aligned} \tag{21}$$

From the above expressions, the Feynman rules can be derived by expanding $U = exp(i\Phi/F)$ everywhere in $\mathcal{L} = \mathcal{L}^{(2)} + \mathcal{L}^{(4)} + \mathcal{L}^{(6)}$ and identifying the relevant vertex monomials. In the next section we display the main result of the two-loop calculations for the form factors.

4 The Form Factors

To $O(p^6)$, the finite matrix elements in ChPT are obtained by multiplying the unrenormalized Feynman diagrams obtained from $\mathcal{L} = \mathcal{L}^{(2)} + \mathcal{L}^{(4)} + \mathcal{L}^{(6)}$ with a factor $\sqrt{Z}$ per external meson, where Z is the wave function renormalization constant. To get these results, we start to calculate the mass and wave function renormalizations as well as that of the pion decay constant.

Since the form factors at $O(p^4)$ are related to the finite counterterm contribution, we only need the wave function renormalization, $m_{K,\pi}^2$ and $F_{K,\pi}$ to $O(p^4)$ in our calculations. Explicitly, we have

$$Z_\pi^{-1} = 1 - \frac{1}{3F^2}\left[I(m_K^2) + 2I(m_\pi^2) - 24(2m_K^2 + m_\pi^2)L_4 - 24m_\pi^2 L_5\right]\,, \tag{22}$$

$$Z_K^{-1} = 1 - \frac{1}{4F^2}\left[I(m_\eta^2) + 2I(m_K^2) + I(m_\pi^2) - 32(2m_K^2 + m_\pi^2)L_4 - 32m_K^2 L_5\right]\,, \tag{23}$$

$$
\begin{aligned}
\delta m_\pi &= \frac{1}{6F^2}\Big[-m_\pi^2 I(m_\eta^2) + 3m_\pi^2 I(m_\pi^2) - 48m_\pi^2(2m_K^2+m_\pi^2)L_4 - 48L_5 m_\pi^4 \\
&\quad +96L_6 m_\pi^2(2m_K^2+m_\pi^2) + 96L_8 m_\pi^4\Big]\ , \qquad (24)\\
\delta m_K &= \frac{1}{12F^2}\Big[4m_K^2 I(m_\eta^2) - 96L_4 m_K^2(2m_K^2+m_\pi^2) - 96L_5 m_K^4 + 192L_8 m_K^4 \\
&\quad +192L_6 m_K^2(2m_K^2+m_\pi^2)\Big]\ , \qquad (25)\\
F_\pi &= F\left\{1+\frac{1}{F^2}\left[-\frac{1}{2}I(m_K^2) - I(m_\pi^2) + 4(2m_K^2+m_\pi^2)L_4 + 4m_\pi^2 L_5\right]\right\}\ , \qquad (26)\\
F_K &= F\left\{1+\frac{1}{F^2}\Big[-\frac{3}{8}I(m_\eta^2) - \frac{3}{4}I(m_K^2) - \frac{3}{8}I(m_\pi^2) + 4(2m_K^2+m_\pi^2)L_4 \right.\\
&\quad \left. +4m_K^2 L_5\Big]\right\}\ , \qquad (27)
\end{aligned}
$$

where

$$
I(m^2) \equiv \mu^{4-D}\int\frac{d^Dq}{(2\pi)^D}\frac{i}{q^2-m^2} = -\frac{m^2}{16\pi^2}\left[\frac{1}{\varepsilon}+1+\ln(4\pi)-\gamma-\ln\left(\frac{m^2}{\mu^2}\right)\right] \qquad (28)
$$

is the standard tadpole integral. It should be noted that the renormalization constants $\delta m(\equiv m_{phys}-m)$ and $\delta F_{K,\pi}(\equiv F_{K,\pi}-F)$ defined above are finite. The divergences and scale dependences of the loop integrals are cancelled by similar factors for L_i in $\mathcal{L}^{(4)}$.

4.1 The vector form factors F_V

Using the chiral Lagrangians mentioned above, one immediately obtains the tree-level contribution for the anomalous parts of our processes. For the semileptonic radiative K decays, we have

$$
F_{V,K,tree} = \frac{1}{4\sqrt{2}\pi^2 F}\left[1 - \frac{256}{3}\pi^2 m_K^2 C_7^W + 256\pi^2(m_K^2-m_\pi^2)C_{11}^W + \frac{64}{3}\pi^2(q^2+k^2)C_{22}^W\right]\ . \qquad (29)
$$

Loop corrections to the above tree-level contribution proceed through diagrams involving at least one vertex given by the WZ lagrangian. As shown in Figure 1 with $P=K$, due to the initial order, most one-loop diagrams can contribute to F_V to $O(p^6)$ constructed with one vertex coming from the WZ Lagrangian and another one from the lowest order chiral lagrangian. Performing the calculation in the three-flavor case, we get

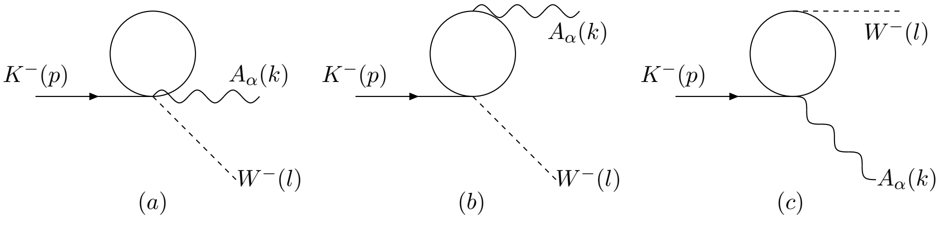

Figure 1: One-loop diagrams that contribute to F_V in $P_{\ell 2\gamma}$

$$
F_{V,K,loop(a)} = \frac{1}{4\sqrt{2}\pi^2 F}\cdot\frac{1}{16\pi^2(\sqrt{2}F)^2}\Big[\lambda(m_\eta^2+2m_K^2+3m_\pi^2)
$$

$$
- m_\eta^2 \ln\left(\frac{m_\eta^2}{\mu^2}\right) - 2m_K^2 \ln\left(\frac{m_K^2}{\mu^2}\right) - 3m_\pi^2 \ln\left(\frac{m_\pi^2}{\mu^2}\right)\Bigg] ,
$$

$$
\begin{aligned}
F_{V,K,loop(b)} = \frac{1}{4\sqrt{2}\pi^2 F} \cdot \frac{1}{16\pi^2(\sqrt{2}F)^2} \Bigg[&(-4m_\pi^2 + \frac{2}{3}k^2)\lambda \\
&+ 4\int (m_\pi^2 - x(1-x)k^2) \ln\left(\frac{m_\pi^2 - x(1-x)k^2}{\mu^2}\right)\Bigg] ,
\end{aligned}
$$

$$
\begin{aligned}
F_{V,K,loop(c)} &= \frac{1}{4\sqrt{2}\pi^2 F} \cdot \frac{1}{16\pi^2(\sqrt{2}F)^2} \Bigg[(-m_\pi^2 - m_\eta^2 - 2m_K^2 + \frac{2}{3}q^2)\lambda \\
&+2\int (xm_\eta^2 + (1-x)m_K^2 - x(1-x)q^2) \ln\left(\frac{xm_\eta^2 + (1-x)m_K^2 - x(1-x)q^2}{\mu^2}\right) dx \\
&+2\int (xm_\pi^2 + (1-x)m_K^2 - x(1-x)q^2) \ln\left(\frac{xm_\pi^2 + (1-x)m_K^2 - x(1-x)q^2}{\mu^2}\right) dx\Bigg] , \quad (30)
\end{aligned}
$$

from the three loops in Figure 1, respectively, where

$$
\lambda = \frac{1}{\varepsilon} + 1 + \ln(4\pi) - \gamma \, . \quad (31)
$$

Putting all of the contributions together as well as the usual renormalizations of the pseudoscalar wave-functions and decay constants, we obtain the following results:

$$
\begin{aligned}
F_{V,K} &= \frac{1}{4\sqrt{2}\pi^2 F_K} \Bigg\{1 - \frac{256}{3}\pi^2 m_K^2 C_7 + 256\pi^2(m_K^2 - m_\pi^2)C_{11} + \frac{64}{3}\pi^2(q^2 + k^2)C_{22} \\
&+\frac{1}{16\pi^2(\sqrt{2}F_K)^2} \Bigg[\frac{5}{3}(m_K^2 - m_\pi^2)\lambda + \frac{2}{3}(k^2 + q^2)\lambda - \frac{3}{2}m_\eta^2 \ln\left(\frac{m_\eta^2}{\mu^2}\right) - 3m_K^2 \ln\left(\frac{m_K^2}{\mu^2}\right) \\
&-\frac{7}{2}m_\pi^2 \ln\left(\frac{m_\pi^2}{\mu^2}\right) + 4\int \Big[m_\pi^2 - x(1-x)k^2\Big] \ln\left(\frac{m_\pi^2 - x(1-x)k^2}{\mu^2}\right) \\
&+2\int \Big[xm_\pi^2 + (1-x)m_K^2 - x(1-x)q^2\Big] \ln\left(\frac{xm_\pi^2 + (1-x)m_K^2 - x(1-x)q^2}{\mu^2}\right) \\
&+2\int \Big[xm_\eta^2 + (1-x)m_K^2 - x(1-x)q^2\Big] \ln\left(\frac{xm_\eta^2 + (1-x)m_K^2 - x(1-x)q^2}{\mu^2}\right)\Bigg]\Bigg\} . \quad (32)
\end{aligned}
$$

Similarly, for $\pi_{l2\gamma}$ we derive

$$
\begin{aligned}
F_{V,\pi} &= \frac{1}{4\sqrt{2}\pi^2 F_\pi} \Bigg\{1 - \frac{256}{3}\pi^2 m_\pi^2 C_7 + \frac{64}{3}\pi^2(q^2 + k^2)C_{22} + \frac{1}{16\pi^2(\sqrt{2}F_\pi)^2}\Big[\\
&-4m_K^2 \ln\frac{m_K^2}{\mu^2} - 4m_\pi^2 \ln\frac{m_\pi^2}{\mu^2} + 4\int (m_K^2 - x(1-x)k^2) \ln\frac{m_K^2 - x(1-x)k^2}{\mu^2} \\
&+4\int (m_\pi^2 - x(1-x)q^2) \ln\frac{m_\pi^2 - x(1-x)q^2}{\mu^2} + \frac{2}{3}(k^2 + q^2)\lambda\Bigg]\Bigg\} . \quad (33)
\end{aligned}
$$

We note that the numerical results of Eqs. (32) and (33) agree with those in Ref. [23] as will be shown in Sec. 6. The one-loop corrections contain divergent terms proportional to $\lambda = \frac{1}{\varepsilon} + 1 + \ln(4\pi) - \gamma$ coming from the dimensional regularization scheme. Obviously, the presence of these divergent terms requires the introduction of the corresponding counterterms in the anomalous section of the Lagrangian at $O(p^6)$, which were already given in Refs. [20, 30, 31]. Their infinite parts cancel the λ-terms in Eqs. (32) and (33) and the coefficients C_i^W are simply substituted for by the remaining finite parts, the renormalized coefficients C_i^{Wr}. The values of these finite contributions from the counterterms to our processes are not pinned down in ChPT and they have to be deduced from data fitting [29] or, alternatively, from the hypothesis of resonance saturation (RS) of the counterterms [23]. The estimations of using RS are described in Sec. 6.

4.2 The axial-vector form factors F_A

In this subsection we aim at the extraction of the form factor F_A, which is the only one that has a contribution proportional to $g_{\mu\nu}(p\cdot k)$. The presence of $g_{\mu\nu}$ requires that the axial-vector and vector insertions are in the same one-particle irreducible subdiagrams. This immediately removes a large part of the diagrams. Furthermore, the $(p\cdot k)$ kinematical factor guarantees that it is not part of the internal Bremsstrahlung contribution. We now discuss the contributions from the diagrams to $O(p^6)$.

4.2.1 Tree-level diagrams

With the chiral Lagrangians in Eqs. (13), (14) and (16), one obtains tree-level contributions for the processes as follows:

$$\begin{aligned}
F^{(4)}_{A,\pi,tree} &= \frac{4\sqrt{2}}{F}(L_9+L_{10})\,, && (34)\\
F^{(4)}_{A,K,tree} &= \frac{4\sqrt{2}}{F}(L_9+L_{10})\,, && (35)\\
F^{(6)}_{A,\pi,tree} &= -y_{17}\frac{48\sqrt{2}m_\pi^2}{F} - y_{18}\frac{48\sqrt{2}(2m_K^2+m_\pi^2)}{F} + y_{81}\frac{16\sqrt{2}m_\pi^2}{F} \\
&\quad + y_{82}\frac{16\sqrt{2}(2m_K^2+m_\pi^2)}{F} - y_{83}\frac{16\sqrt{2}m_\pi^2}{F} - y_{84}\frac{8\sqrt{2}(2m_K^2+m_\pi^2)}{F} \\
&\quad - y_{85}\frac{8\sqrt{2}m_\pi^2}{F} + y_{100}\frac{8\sqrt{2}(p_\pi^2-p_\pi\cdot k)}{F} - y_{102}\frac{16\sqrt{2}m_\pi^2}{F} \\
&\quad - y_{103}\frac{16\sqrt{2}(2m_K^2+m_\pi^2)}{F} + y_{104}\frac{16\sqrt{2}m_\pi^2}{F} + y_{109}\frac{8\sqrt{2}(2p_\pi\cdot k-p_\pi^2)}{F} \\
&\quad - y_{110}\frac{4\sqrt{2}p_\pi\cdot k}{F}\,, && (36)\\
F^{(6)}_{A,K,tree} &= -y_{17}\frac{48\sqrt{2}m_K^2}{F} - y_{18}\frac{48\sqrt{2}(2m_K^2+m_\pi^2)}{F} + y_{81}\frac{16\sqrt{2}(2m_K^2+m_\pi^2)}{3F} \\
&\quad + y_{82}\frac{16\sqrt{2}(2m_K^2+m_\pi^2)}{F} - y_{83}\frac{16\sqrt{2}(2m_K^2+m_\pi^2)}{3F} \\
&\quad - y_{84}\frac{8\sqrt{2}(2m_K^2+m_\pi^2)}{F} - y_{85}\frac{8\sqrt{2}(4m_K^2-m_\pi^2)}{3F} \\
&\quad + y_{100}\frac{8\sqrt{2}(p_K^2-p_K\cdot k)}{F} - y_{102}\frac{16\sqrt{2}m_K^2}{F} - y_{103}\frac{16\sqrt{2}(2m_K^2+m_\pi^2)}{F} \\
&\quad + y_{104}\frac{16\sqrt{2}m_K^2}{F} + y_{109}\frac{8\sqrt{2}(2p_K\cdot k-p_K^2)}{F} - y_{110}\frac{4\sqrt{2}p_K\cdot k}{F}\,. && (37)
\end{aligned}$$

We note that for the tree-level contributions in Eqs. (36) and (37) at $O(p^6)$ one needs to perform renormalization with the finite parts, which will be discussed in Sec. 5.

4.2.2 One-loop diagrams

We now consider the one-loop diagrams shown in Figure 1. Since it contains only photon-even-meson vertices in the non-anomalous chiral lagrangian to $O(p^4)$, Figure 1(c) does not contribute to F_A. Moreover, one-loop diagrams with an $O(p^4)$ vertex insertion on a propagator in the loop never produce the factor $(p \cdot k)$ and hence do not contribute to F_A. From Figures 1(a) and 1(b), we get

$$\begin{aligned}
F_{A,\pi,loop(a)} &= -\frac{L_9}{3F^3}\left[14\sqrt{2}I(m_K^2) + 28\sqrt{2}I(m_\pi^2)\right] \\
&\quad -\frac{2L_{10}}{3F^3}\left[10\sqrt{2}I(m_K^2) + 20\sqrt{2}I(m_\pi^2)\right] , \\
F_{A,K,loop(a)} &= -\frac{L_9}{3F^3}\left[6\sqrt{2}I(m_\eta^2) + 24\sqrt{2}I(m_K^2) + 12\sqrt{2}I(m_\pi^2)\right] \\
&\quad -\frac{2L_{10}}{3F^3}\left[3\sqrt{2}I(m_\eta^2) + 18\sqrt{2}I(m_K^2) + 9\sqrt{2}I(m_\pi^2)\right] , \\
F_{A,\pi,loop(b)} &= \frac{-16\sqrt{2}L_1}{F^3}I(m_\pi^2) + \frac{8\sqrt{2}L_2}{F^3}I(m_\pi^2) - \frac{8\sqrt{2}L_3}{F^3}\left[I(m_\pi^2) + \frac{1}{2}I(m_K^2)\right] \\
&\quad -\frac{2\sqrt{2}L_9}{F^3}\left[I(m_K^2) + 2I(m_\pi^2)\right] , \\
F_{A,K,loop(b)} &= \frac{-16\sqrt{2}L_1}{F^3}I(m_K^2) + \frac{8\sqrt{2}L_2}{F^3}I(m_K^2) - \frac{8\sqrt{2}L_3}{F^3}\left[I(m_K^2) + \frac{1}{2}I(m_\pi^2)\right] \\
&\quad -\frac{2\sqrt{2}L_9}{F^3}\left[I(m_\pi^2) + 2I(m_K^2)\right] . \qquad (38)
\end{aligned}$$

4.2.3 Two-loop diagrams

The two-loop diagrams which may contribute to F_A are shown in Figure 2. The last six diagrams with nonoverlapping loops in Figure 2, which can be written as the products of one-loop integrals and produce no $(p \cdot k)$ factor, do not contribute to F_A. The only possible non-vanishing diagrams are the first three irreducible ones in Figure 2.

Since there are three different mass scales of (m_π, m_K, m_η) with the same order of magnitude in the $SU(3)$ ChPT, the irreducible integrals can no longer be expressed by elementary analytical functions. We will quote only the numerical results in Sec. 5 and Sec. 6. We now give the detailed calculations for the $g_{\mu\nu}$ terms of M_A in Eq. (5). It is clear that the first irreducible diagram in Figure 2 does not contribute to F_A since there is no $(p \cdot k)$ term. The second and third irreducible diagrams with genuine massive two-loop integrals [21] are depicted in Figures 3 and 4, respectively. Our calculations on these diagrams are summarized in Appendix A.

We point out that the two-point irreducible diagrams in Figure 3 vanished in Ref. [24] for $\pi_{\ell 2\gamma}$ in the linear sigma model parametrization in which there is neither a photon nor a four-pion vertex [32]. As shown in Sec. 5, these diagrams play a very important role in the cancellation of divergent parts with $1/\epsilon^2$ in the final results.

We note that the two-loop amplitudes shown in Appendix A have been classified by the functions $\{I, II..., A, B...L\}$ related to each diagram. For clarity, we always refer to all

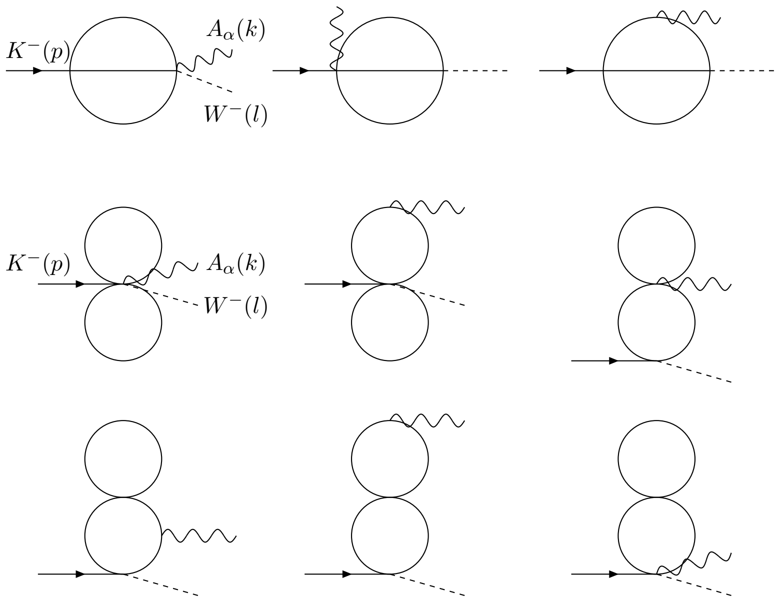

Figure 2: Two-loop diagrams for the form factors in $P_{\ell 2\gamma}$.

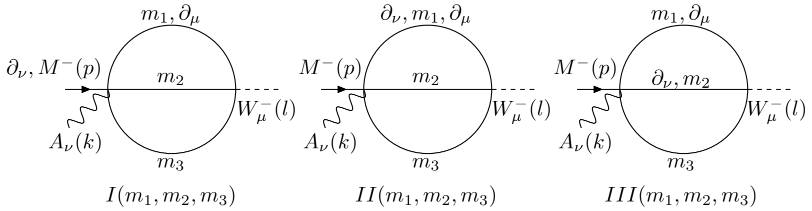

Figure 3: Two-point irreducible diagrams

inward particles for vertices. The Feynman diagrams which contain tensor structures at the numerator can be reduced to the calculation of scalar integrals $P^{ab}_{\alpha 1,\alpha 2,\alpha 3}$ by introducing the transverse components of the loop momenta s and q as $s^\mu_\perp = s^\mu - (s \cdot l/l^2)l^\mu$ and $q^\mu_\perp = q^\mu - (q \cdot l/l^2)l^\mu$, respectively, for the two-point diagrams [21]. For the three-point diagrams, we first combine the denominators by using the Feynman formula $1/ab = \int_0^1 dx/[ax + b(1-x)]^2$ and then replace l by $l' = l + kx$, i.e., $s^\mu_\perp = s^\mu - (s \cdot l'/l'^2)l'^\mu$ and $q^\mu_\perp = q^\mu - (q \cdot l'/l'^2)l'^\mu$. The corresponding relations among $\{I, II..., A, B...L\}$ and $P^{ab}_{\alpha 1,\alpha 2,\alpha 3}$ are displayed in Appendices B and C , where the scalar integrals $P^{ab}_{\alpha 1,\alpha 2,\alpha 3}$, defined in the Euclidian space, are given by

$$P^{ab}_{\alpha 1,\alpha 2,\alpha 3}(m_1, m_2, m_3; l^2) = \int d^n s d^n q \frac{(s \cdot l)^a (q.l)^b}{(s^2 + m_1^2)^{\alpha 1}(q^2 + m_2^2)^{\alpha 2}((s+q)^2 + m_3^2)^{\alpha 1}} \, . \qquad (39)$$

The detailed contributions from all diagrams for F_A in $\pi_{\ell 2\gamma}$ and $K_{\ell 2\gamma}$ are summarized in the next section.

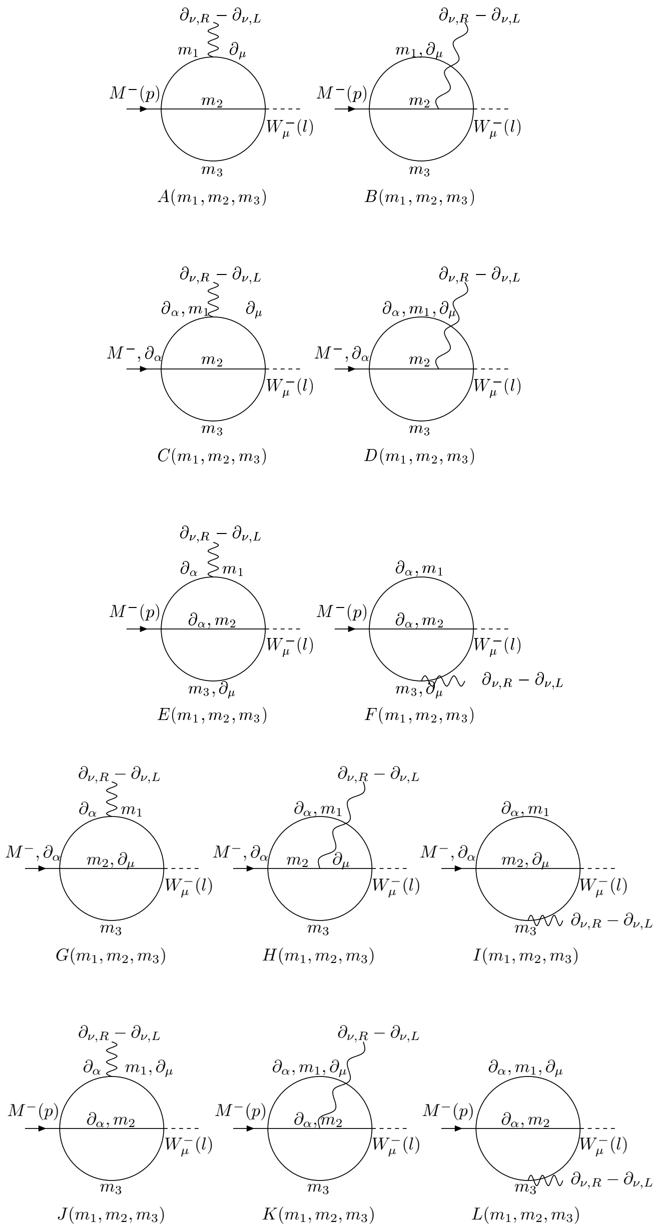

Figure 4: Three-point irreducible diagrams

5 Analytical Results

5.1 Renormalization scheme

In our calculations, we use the following dimensional regularization and renormalization scheme [1, 2, 22, 28]. Each diagram of $O(p^{2n})$ is multiplied by a factor $(c\mu)^{(n-1)(D-4)}$, where $D = 4 - 2\epsilon$ is the dimension of space-time and c is given by

$$\ln c = -\frac{1}{2}\left[1 - \gamma + \ln(4\pi)\right] - \frac{\epsilon}{2}\left(\frac{\pi^2}{12} + \frac{1}{2}\right) + O(\epsilon^2)\,. \tag{40}$$

Using the renormalization factor of $(c\mu)^{(n-1)(D-4)}$, the low energy constants L_i of $\mathcal{L}_n^{(4)}$ in Eq. (14) are defined by

$$L_i = (c\mu)^{(D-4)} L_i(\mu, D) \, . \tag{41}$$

Similarly, for the $\mathcal{L}_n^{(6)}$ parameters y_i in Eq. (16),

$$y_i = (c\mu)^{2(D-4)} y_i(\mu, D) \, . \tag{42}$$

We note that $L_i(\mu, D)$ have the same μ-dependences as the one-loop integrals, whereas $y_i(\mu, D)$ behave like the two-loop ones. Their values at the two different scales of μ_1 and μ_2 are related by $L_i(\mu_1, D) = (\mu_2/\mu_1)^{(D-4)} L_i(\mu_2, D)$ and $y_i(\mu_1, D) = (\mu_2/\mu_1)^{2(D-4)} y_i(\mu_2, D)$, respectively.

5.2 Analytical forms of F_A

We now try to obtain the analytical forms of F_A from each diagram to $O(p^6)$ at the scale of m_ρ. From Sec. 5.1, for the unrenormalized coefficients in the chiral lagrangian $\mathcal{L}_n^{(4)}$, we use [22, 28]

$$\begin{aligned} L_i &= (c\mu)^{(D-4)} \left[-\frac{\gamma_i}{32\pi^2 \epsilon} + L_i^r(\mu) \right] \\ &= \mu^{(D-4)} \left\{ -\frac{\gamma_i}{32\pi^2} \left[\frac{1}{\epsilon} - \gamma_s - \ln\left(\frac{m_\rho^2}{\mu^2} \right) \right] + L_i^r(m_\rho) + \epsilon L_i^{(\epsilon)}(m_\rho, \mu) \right\} \, , \end{aligned} \tag{43}$$

which is a Laurent series expanded around $\epsilon = 0$. Of the values in Eq. (43), γ_i are shown in Table 1 [22], $\gamma_s = -1 - \ln(4\pi) + \gamma$, L_i^r correspond to measurable low energy constants and $L_i^{(\epsilon)}$ are given by $L_i^{(\epsilon)}(m_\rho, \mu) = -L_i^r(m_\rho)(\gamma_s + \ln(m_\rho^2/\mu^2)) + \gamma_i \cdot f(m_\rho, \mu)$. Similarly, for the chiral lagrangian $\mathcal{L}_n^{(6)}$, we have

Table 1: Coefficients of γ_i in the Minkowski space [22].

i	1	2	3	4	5	6	7	8	9	10
γ_i	$\frac{3}{32}$	$\frac{3}{16}$	0	$\frac{1}{8}$	$\frac{3}{8}$	$\frac{11}{144}$	0	$\frac{5}{48}$	$\frac{1}{4}$	$\frac{-1}{4}$

$$\begin{aligned} y_i &= \frac{(c\mu)^{2(D-4)}}{F^2} \left\{ y_i^r(\mu) + \left[\Gamma_i^{(1)} + \Gamma_i^{(L)}(\mu) \right] \frac{1}{32\pi^2 \epsilon} - \Gamma_i^{(2)} \frac{1}{32^2 \pi^4 \epsilon^2} \right\} \\ &= \frac{\mu^{2(D-4)}}{F^2} \left\{ y_i^r(m_\rho) + \frac{\left(\Gamma_i^{(1)} + \Gamma_i^{(L)}(m_\rho) \right)}{32\pi^2} \left[\frac{1}{\epsilon} - 2\gamma_s - 2\ln\left(\frac{m_\rho^2}{\mu^2} \right) \right] - \Gamma_i^{(2)} \frac{g(m_\rho, \mu, \epsilon)}{32^2 \pi^4 \epsilon^2} \right\} \, ; \end{aligned} \tag{44}$$

the relevant constants of $\Gamma_i^{(1)}$, $\Gamma_i^{(2)}$ and $\Gamma_i^{(L)}$ are shown in Table 2 [22]. We note that $f(m_\rho, \mu)$ and $g(m_\rho, \mu, \epsilon)$, which receive contributions from the $(\epsilon/2)$ term in Eq. (40), will not contribute to F_A.

By writing the unrenormalized contributions to F_A of $O(p^4)$ and $O(p^6)$ diagrams as $F_{A,tree}(p^4)$, $F_{A,tree}(p^6)$, $F_{A,1-loop}(p^6)$ and $F_{A,2-loop}(p^6)$, respectively, using the wave function renormalizations, we find

$$F_A = \sqrt{Z_P} \left[F_{A,tree}(p^4)(1 + \delta F_P) + F_{A,tree}(p^6) + F_{A,1-loop}(p^6) + F_{A,2-loop}(p^6) \right] \, , \tag{45}$$

Table 2: Coefficients of $\Gamma_i^{(2)}$ and $\Gamma_i^{(1,L)}$ with the double-pole and single-pole divergences, respectively, in the Minkowski space [22].

y_i	$\Gamma_i^{(2)}$	$16\pi^2\Gamma_i^{(1)}$	$\Gamma_i^{(L)}$
17	$\frac{19}{64}$	$-\frac{13}{768}$	$\frac{2}{3}L_1^r + \frac{4}{3}L_2^r + \frac{8}{9}L_3^r + \frac{3}{4}\text{Ł}_5^r$
18	$\frac{67}{192}$	$-\frac{1}{2304}$	$\frac{8}{3}L_1^r + \frac{8}{9}L_2^r + \frac{23}{27}L_3^r + \frac{3}{2}\text{Ł}_4^r + \frac{1}{4}L_5^r$
81	0	0	$-\frac{3}{4}L_9^r - \frac{3}{4}L_{10}^r$
82	0	0	$-\frac{1}{4}L_9^r - \frac{1}{4}\text{Ł}_{10}^r$
83	$-\frac{1}{4}$	$\frac{5}{384}$	$\frac{1}{3}L_1^r - \frac{11}{6}L_2^r - \frac{5}{36}L_3^r - \frac{3}{4}L_5^r + \frac{3}{8}L_9^r$
84	$-\frac{4}{3}$	$-\frac{5}{144}$	$-\frac{32}{3}L_1^r - \frac{32}{9}L_2^r - \frac{157}{54}L_3^r - 6L_4^r - \text{Ł}_5^r + \frac{1}{2}L_9^r$
85	$-\frac{1}{2}$	$\frac{5}{192}$	$\frac{2}{3}L_1^r - \frac{11}{3}L_2^r - \frac{16}{9}L_3^r - \frac{3}{2}L_5^r + \frac{3}{4}L_9^r$
100	$-\frac{5}{24}$	$\frac{49}{1152}$	$\frac{1}{3}L_1^r - \frac{1}{6}L_2^r + \frac{1}{4}L_3^r - \frac{1}{3}\text{Ł}_4^r - \frac{1}{4}L_5^r - \frac{9}{8}L_9^r$
102	$-\frac{25}{64}$	$-\frac{17}{768}$	$-\frac{2}{3}L_1^r - \frac{4}{3}L_2^r - \frac{8}{9}L_3^r - \frac{3}{4}\text{Ł}_5^r + \frac{3}{4}L_{10}^r$
103	$-\frac{73}{192}$	$-\frac{101}{2304}$	$-\frac{8}{3}L_1^r - \frac{8}{9}L_2^r - \frac{23}{27}L_3^r - \frac{3}{2}L_4^r - \frac{1}{4}L_5^r + \frac{1}{4}L_{10}^r$
104	$\frac{7}{96}$	$\frac{5}{144}$	$-\frac{1}{6}L_1^r + \frac{1}{12}L_2^r - \frac{1}{8}L_3^r + \frac{1}{6}\text{Ł}_4^r + \frac{1}{8}L_5^r + \frac{5}{16}L_9^r$
109	$-\frac{1}{16}$	$\frac{3}{128}$	$-\frac{1}{2}L_9^r$
110	$\frac{1}{6}$	$-\frac{31}{576}$	$-\frac{2}{3}L_1^r + \frac{1}{3}L_2^r - \frac{1}{2}L_3^r + \frac{2}{3}\text{Ł}_4^r + \frac{1}{2}L_5^r + \frac{1}{4}L_9^r$

which leads to

$$F_A \;=\; F_{A,tree}(p^4)(1+\delta F_P+\frac{1}{2}\delta Z_P)+F_{A,tree}(p^6)+F_{A,1-loop}(p^6)+F_{A,2-loop}(p^6)\,, \tag{46}$$

where $P=\pi$ or K. In Eq. (46), for $P=\pi$, we have

$$\begin{aligned}
F_{A,tree}(1+\delta F_\pi+\frac{1}{2}\delta Z_\pi) &= \frac{4\sqrt{2}}{F_\pi}\left(L_9^r+L_{10}^r\right)\left[1-\frac{1}{F^2}\left(\frac{I(m_K^2)}{3}+\frac{2I(m_\pi^2)}{3}\right)\right]\\
&= \frac{4\sqrt{2}}{F_\pi}\left(L_9^r+L_{10}^r\right)\left\{1+\frac{1}{16\pi^2F_\pi^2}\left[\frac{1}{\varepsilon}-2\gamma_s-2\ln(\frac{m_\rho^2}{\mu^2})\right]\left(\frac{m_K^2}{3}+\frac{2m_\pi^2}{3}\right)\right.\\
&\qquad\left.-\frac{1}{16\pi^2F_\pi^2}\left[\frac{m_K^2}{3}\ln\left(\frac{m_K^2}{m_\rho^2}\right)+\frac{2m_\pi^2}{3}\ln\left(\frac{m_\pi^2}{m_\rho^2}\right)\right]\right\}\,,
\end{aligned} \tag{47}$$

$$\begin{aligned}
F_{A,1-loop} \;=\;& \frac{1}{6\sqrt{2}F_\pi^3\pi^2}\left[\frac{1}{\epsilon}-2\gamma_s-2\ln\left(\frac{m_\rho^2}{\mu^2}\right)\right]\times\\
&\left[6(2L_1^r-L_2^r)m_\pi^2+(m_K^2+2m_\pi^2)(3L_3^r+5L_9^r+5L_{10}^r)\right]\\
&+\frac{1}{6\sqrt{2}F_\pi^3\pi^2}\left\{(-12L_1^r+6L_2^r)m_\pi^2\ln\left(\frac{m_\pi^2}{m_\rho^2}\right)-(3L_3^r+5L_9^r+5L_{10}^r)\times\right.\\
&\left.\left[m_K^2\ln\left(\frac{m_K^2}{m_\rho^2}\right)+2m_\pi^2\ln\left(\frac{m_\pi^2}{m_\rho^2}\right)\right]\right\}\,,
\end{aligned} \tag{48}$$

$$F_{A,2-loop} \;=\; \frac{1}{6F_\pi^3(2\pi)^8}\left\{-\frac{\pi^4(116m_K^2+184m_\pi^2+21m_\eta^2)}{12\sqrt{2}}\left[\frac{1}{\epsilon}-2\gamma_s-2\ln\left(\frac{m_\rho^2}{\mu^2}\right)\right]\right.$$

$$
\begin{aligned}
& -\frac{3\pi^4}{2\sqrt{2}}\left[\frac{1}{\epsilon}-2\gamma_s-2\ln\left(\frac{m_\rho^2}{\mu^2}\right)\right](p\cdot k) \\
& -1421.4-1167.7(p\cdot k)+1228.0+1123.2(p\cdot k)\Big\}\ , \qquad (49)
\end{aligned}
$$

$$
\begin{aligned}
F_{A,tree}(p^6) \;=\; & -\left[\frac{1}{\epsilon}-2\gamma_s-2\ln\left(\frac{m_\rho^2}{\mu^2}\right)\right]\Big\{-\frac{1}{6F_\pi^3(2\pi)^8}\frac{3\pi^4}{2\sqrt{2}}(p\cdot k) \\
& -\frac{1}{6F_\pi^3(2\pi)^8}\frac{\pi^4(432m_K^2+531m_\pi^2)}{36\sqrt{2}}+\frac{1}{6\sqrt{2}F_\pi^3\pi^2}\Big[3m_K^2(L_3^r+2L_9^r+2L_{10}^r) \\
& +6m_\pi^2(2L_1^r-L_2^r+L_3^r+2L_9^r+2L_{10}^r)\Big]\Big\} \\
& -\frac{4\sqrt{2}}{F_\pi^3}\Big\{4m_K^2(6y_{18}^r-2y_{82}^r+y_{84}^r+2y_{103}^r) \\
& +2m_\pi^2(6y_{17}^r+6y_{18}^r-2y_{81}^r-2y_{82}^r+2y_{83}^r+y_{84}^r+y_{85}^r-y_{100}^r+2y_{102}^r \\
& +2y_{103}^r-2y_{104}^r+y_{109}^r)+pk(2y_{100}^r-4y_{109}^r+y_{110}^r)\Big\}\ . \qquad (50)
\end{aligned}
$$

For $P=K$, we get

$$
\begin{aligned}
& F_{A,tree}(1+\delta F_K+\frac{1}{2}\delta Z_K)=\frac{4\sqrt{2}}{F_K}(L_9^r+L_{10}^r)\left[1-\frac{1}{F^2}\left(\frac{I(m_\eta^2)}{4}+\frac{I(m_K^2)}{2}+\frac{I(m_\pi^2)}{4}\right)\right] \\
& \quad =\frac{4\sqrt{2}}{F_K}(L_9^r+L_{10}^r)\left\{1+\frac{1}{16\pi^2F_K^2}\left[\frac{1}{\varepsilon}-2\gamma_s-2\ln\left(\frac{m_\rho^2}{\mu^2}\right)\right]\left(\frac{m_\eta^2}{4}+\frac{m_K^2}{2}+\frac{m_\pi^2}{4}\right)\right. \\
& \qquad \left.-\frac{1}{16\pi^2F_K^2}\left[\frac{m_\eta^2}{4}\ln\left(\frac{m_\eta^2}{m_\rho^2}\right)+\frac{m_K^2}{2}\ln\left(\frac{m_K^2}{m_\rho^2}\right)+\frac{m_\pi^2}{4}\ln\left(\frac{m_\pi^2}{m_\rho^2}\right)\right]\right\}\ , \qquad (51)
\end{aligned}
$$

$$
\begin{aligned}
F_{A,1-loop} \;=\; & \frac{1}{4\sqrt{2}F_K^3\pi^2}\left[\frac{1}{\epsilon}-2\gamma_s-2\ln\left(\frac{m_\rho^2}{\mu^2}\right)\right]\Big\{m_K^2(8L_1^r-4L_2^r+4L_3^r+6L_9^r+6L_{10}^r) \\
& +m_\pi^2(2L_3^r+3L_9^r+3L_{10}^r)+m_\eta^2(L_9^r+L_{10}^r)\Big\} \\
& +\frac{1}{4\sqrt{2}F_K^3\pi^2}\left\{-(2L_3^r+3L_9^r+3L_{10}^r)m_\pi^2\ln\left(\frac{m_\pi^2}{m_\rho^2}\right)-(L_9^r+L_{10}^r)m_\eta^2\ln\left(\frac{m_\eta^2}{m_\rho^2}\right)\right. \\
& \left.-(8L_1^r-4L_2^r+4L_3^r+6L_9^r+6L_{10}^r)m_K^2\ln\left(\frac{m_K^2}{m_\rho^2}\right)\right\}\ , \qquad (52)
\end{aligned}
$$

$$
\begin{aligned}
F_{A,2-loop} \;=\; & \frac{1}{6F_K^3(2\pi)^8}\left\{-\frac{\pi^4(99m_K^2+20m_\pi^2-12m_\eta^2)}{4\sqrt{2}}\left[\frac{1}{\epsilon}-2\gamma_s-2\ln\left(\frac{m_\rho^2}{\mu^2}\right)\right]\right. \\
& -\frac{3\pi^4}{2\sqrt{2}}\left[\frac{1}{\epsilon}-2\gamma_s-2\ln\left(\frac{m_\rho^2}{\mu^2}\right)\right](p\cdot k) \\
& \left.-1465.2-923.0(p\cdot k)+1266.9+1208.3(p\cdot k)\right\}\ , \qquad (53)
\end{aligned}
$$

$$
\begin{aligned}
F_{A,tree}(p^6) \;=\; & -\left[\frac{1}{\epsilon}-2\gamma_s-2\ln\left(\frac{m_\rho^2}{\mu^2}\right)\right]\Big\{-\frac{1}{6F_K^3(2\pi)^8}\frac{3\pi^4}{2\sqrt{2}}(p\cdot k) \\
& -\frac{1}{6F_K^3(2\pi)^8}\frac{\pi^4(747m_K^2+216m_\pi^2)}{36\sqrt{2}}+\frac{1}{4\sqrt{2}F_K^3\pi^2}\Big[m_\pi^2(2L_3^r+3L_9^r+3L_{10}^r)
\end{aligned}
$$

$$
\begin{aligned}
&+m_K^2(8L_1^r - 4L_2^r + 4L_3^r + 9L_9^r + 9L_{10}^r)\Big]\Big\} \\
&-\frac{4\sqrt{2}}{3F_K^3}\Big\{2m_\pi^2(18y_{18}^r - 2y_{81}^r - 6y_{82}^r + 2y_{83}^r + 3y_{84}^r - y_{85}^r + 6y_{103}^r) \\
&+2m_K^2(18y_{17}^r + 36y_{18}^r - 4y_{81}^r - 12y_{82}^r + 4y_{83}^r + 6y_{84}^r + 4y_{85}^r - 3y_{100}^r \\
&+6y_{102}^r + 12y_{103}^r - 6y_{104}^r + 3y_{109}^r) + 3pk(2y_{100}^r - 4y_{109}^r + y_{110}^r)\Big\}\ .
\end{aligned}
\tag{54}
$$

We note that, in the above expressions, one special case must be treated separately. For the finite part of $F_{A,2-loop}$, the functions of $g(y)$ and $f_i(y)$ in Appendix B seem to introduce additional singularities in the integrals, such as at $y = 0$ and 1. However, this problem can be resolved by noticing that at $y = 0$ (the situation is the same at y=1), the function, e.g. $g(y)$, behaves like $\ln(x^2)$, which is integrable. Consequently, the main question of evaluating the finite part of $F_{A,2-loop}$ is how to implement the formula in a computer program by correct and numerically stable forms. As seen from the last two terms for $F_{A,2-loop}$ in Eqs. (49) and (53), we have found the reliable and stable numerical results due to the contributions of functions h_i, i.e., the integrals of g and f_i, by fitting the numerical data with recursive analytic methods.

We remark that in Eqs. (47)-(54) we have explicitly shown the single poles, subtracted via $F_{A,tree}(p^6)$. We emphasize that in our results there are no divergent parts with $1/\epsilon^2$ and all the terms related to $1/\epsilon$ are cancelled explicitly by the renormalization of the coupling constants in $\mathcal{L}_n^{(6)}$ as well as the Gell-Mann-Okubo relation in Eq. (10). It is clear that the disappearance of $1/\epsilon^2$ terms relies on the two-point irreducible diagrams in Figure 3. Moreover, our results are scale independent since the scale terms with $\ln\mu^2$ can be grouped into the ones with $1/\epsilon$, i.e., they are always associated with $1/\epsilon$ terms. These also serve as checks of our calculations. Now we can extract the axial-vector form factor by placing the related physical quantities into the Eq. (46). Explicitly, we may write Eq. (46) into more transparent forms

$$
\begin{aligned}
F_{A,\pi} \;=\;& \{66.86(L_9^r + L_{10}^r)\} \\
&+\{(2.41 - 122.96(pk))\frac{y_{100}^r}{F^2} - 4.82\frac{y_{102}^r}{F^2} - 125.35\frac{y_{103}^r}{F^2} + 4.82\frac{y_{104}^r}{F^2} \\
&+(-2.41 + 245.95(pk))\frac{y_{109}^r}{F^2} - 61.49(pk)\frac{y_{110}^r}{F^2} - 14.46\frac{y_{17}^r}{F^2} - 376.05\frac{y_{18}^r}{F^2} \\
&+4.82\frac{y_{81}^r}{F^2} + 125.35\frac{y_{82}^r}{F^2} - 4.82\frac{y_{83}^r}{F^2} - 62.67\frac{y_{84}^r}{F^2} - 2.41\frac{y_{85}^r}{F^2}\} \\
&+\{12.30L_1^r - 6.15L_2^r + 16.11L_3^r + 26.85L_9^r + 26.85L_{10}^r\} \\
&+\Big\{-1.70\cdot 10^{-2} - 3.92\cdot 10^{-3}(pk)\Big\}
\end{aligned}
\tag{55}
$$

and

$$
\begin{aligned}
F_{A,K} \;=\;& \{54.99(L_9^r + L_{10}^r)\} \\
&+\{(24.75 - 101.01(pk))\frac{y_{100}^r}{F^2} - 49.50\frac{y_{102}^r}{F^2} - 102.97\frac{y_{103}^r}{F^2} + 49.50\frac{y_{104}^r}{F^2} \\
&+(-24.75 + 202.03(pk))\frac{y_{109}^r}{F^2} - 50.50(pk)\frac{y_{110}^r}{F^2} - 148.50\frac{y_{17}^r}{F^2} - 308.90\frac{y_{18}^r}{F^2} \\
&+34.32\frac{y_{81}^r}{F^2} + 102.97\frac{y_{82}^r}{F^2} - 34.32\frac{y_{83}^r}{F^2} - 51.48\frac{y_{84}^r}{F^2} - 32.34\frac{y_{85}^r}{F^2}\}
\end{aligned}
$$

$$+\{22.08L_1^r - 11.04L_2^r + 12.75L_3^r + 21.71L_9^r + 21.71L_{10}^r\}$$
$$+\left\{-0.97\cdot 10^{-2} + 13.93\cdot 10^{-3}(pk)\right\}\,, \tag{56}$$

where the four $\{\cdots\}$ terms in Eqs. (55) and (56) correspond to those in Eq. (46), respectively.

6 Numerical values and conclusions

As shown in section 5, the divergent terms for F_A in loop-diagrams are cancelled by the corresponding counterterms in the Lagrangian at $O(p^6)$. The infinite parts cancel each other and thus they can be simply substituted by the remaining finite part of the counterterms, y_i^r. We now study the finite parts which contain the actual physical information. We will present the results in numerical forms, with the scale at $m_\rho = 0.77\ GeV$. In Table 3, we show the standard values for the couplings L_i^r in $\mathcal{L}_n^{(4)}$ [6] and those in the two-loop calculation of ChPT; we chose the Main Fit in Ref. [33] as an illustration. Other two-loop studies in ChPT can be found in Refs. [34, 35]. We note that in the table the central value of $\alpha_{10}^r = -5.5$ is kept, and our numerical results for F_A are sensitive to this value. Several $O(p^6)$ low-energy constants of the normal chiral Lagrangian have been evaluated from the RS. In Table 4 we illustrate the values of y_i in the lowest meson dominance (LMD) approximation [25] and the resonance Lagrangian (RL) [23, 25, 36].

Table 3: Values of L_i^r in $\mathcal{L}_n^{(4)}$.

$10^3 L_i^r$	1	2	3	9	10
$O(p^4)$ [6]	0.4 ± 0.3	1.35 ± 0.30	-3.5 ± 1.1	6.9 ± 0.7	-5.5 ± 0.7
Main Fit [33]	0.53 ± 0.25	0.71 ± 0.27	-2.72 ± 1.12	6.9 ± 0.7	-5.5 ± 0.7

Table 4: Values of y_i in $\mathcal{L}_n^{(6)}$.

y_i(*in units of* $10^{-4}/F^2$)	y_{100}	y_{104}	y_{109}	y_{110}
LMD	1.09	−0.36	0.40	−0.52
RL I	1.09	−0.29	0.47	−0.16
RL II	1.49	−0.39	0.65	−0.14

To study the vector form factors, we need to consider the anomalous chiral Lagrangian. The set of anomalous coefficients is treated by phenomenological fitting in ChPT as well as by the two main alternative models of vector meson dominance (VMD) method and constituent chiral quark model (CQM) [29]. The relevant terms for our purposes are shown in Table 5. Other physical inputs are $m_K = 0.495$, $m_\pi = 0.14$, $m_\eta = 0.55$, $F_K = 0.112$, $F = 0.0871$ and $F_\pi = 0.092\ GeV$. We note that some of the actual values of F_π and the masses in our calculations may be different from those in the literature. In particular F_π could differ around 1% from one paper to another; however, we expect that the changes

Table 5: Values of C_i^{Wr} in $\mathcal{L}_a^{(6)}$ in various models [29].

$C_i^{Wr}[10^{-3}GeV^{-2}]$	7	11	22
$ChPT$	0.013 ± 1.17 20.3 ± 18.7	-6.37 ± 4.54	6.52 ± 0.78 5.07 ± 0.71
VMD			$\frac{3}{64M_\rho^2\pi^2} \simeq 8.01$
CQM	0.51 ± 0.06	-0.00143 ± 0.03	3.94 ± 0.43

on our $O(p^6)$ results due to the different sets of parameters are less than 5% since $O(p^6)$ contributions are at least proportional to F_π^3.

To compare our results with those in the literature, we use dimensionless form factors of $f_{V,A}$, defined by

$$f_i = m_P F_i\,, \quad (i = V, A) \tag{57}$$

to replace $F_{V,A}$.

In Figures 5 and 6, we plot the dimensionless vector and axial-vector form factors $f_{V,A}$ as functions of q^2 with the photon on mass-shell for $\pi_{e2\gamma}$ and $K_{e2\gamma}$, respectively. Similar figures can also be drawn for the μ modes. In Table 6, we show the form factors of f_A at $q^2 = 0$ at $O(p^4)$ and $O(p^6)$ with $SU(2)$ and $SU(3)$ symmetries as well as experimental values for $P = K$ and π.

Table 6: f_A at $q^2 = 0$ for $P = K$ and π.

$f_A(q^2 = 0)$	$O(p^4)$ [6]	$O(p^6)\|_{SU(2)}$	$O(p^6)\|_{SU(3)}$	*Experiment*
$P = K$	0.041	–	0.034	0.035 ± 0.020 [37, 38]
$P = \pi$	0.0102	0.0117 [24]	0.0112	0.0116 ± 0.0016 [39]

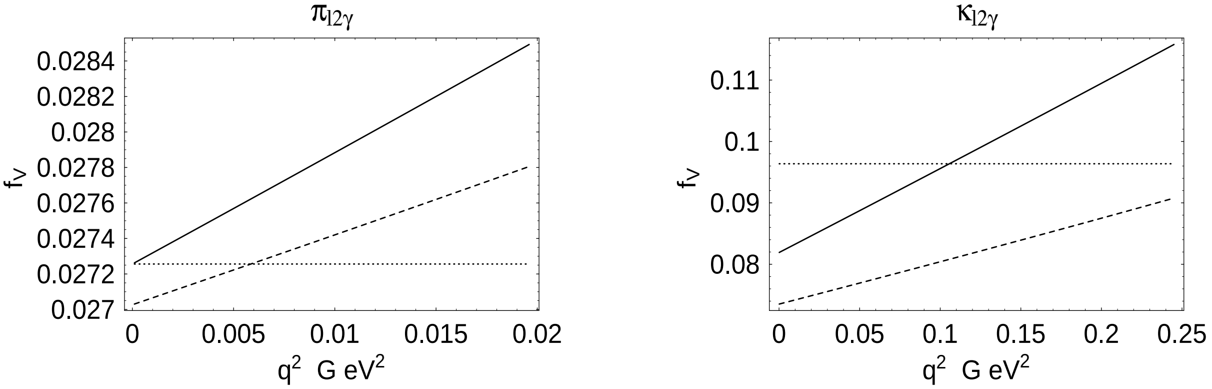

Figure 5: The vector form factors f_V as functions of the momentum transfer q^2 for $\pi_{\ell 2\gamma}$ and $K_{\ell 2\gamma}$ with $\ell = e$. The dot, solid and dashed curves stand for the contributions of $O(p^4)$, $O(p^4) + O(p^6)$ in VMD and $O(p^4) + O(p^6)$ in CQM, respectively.

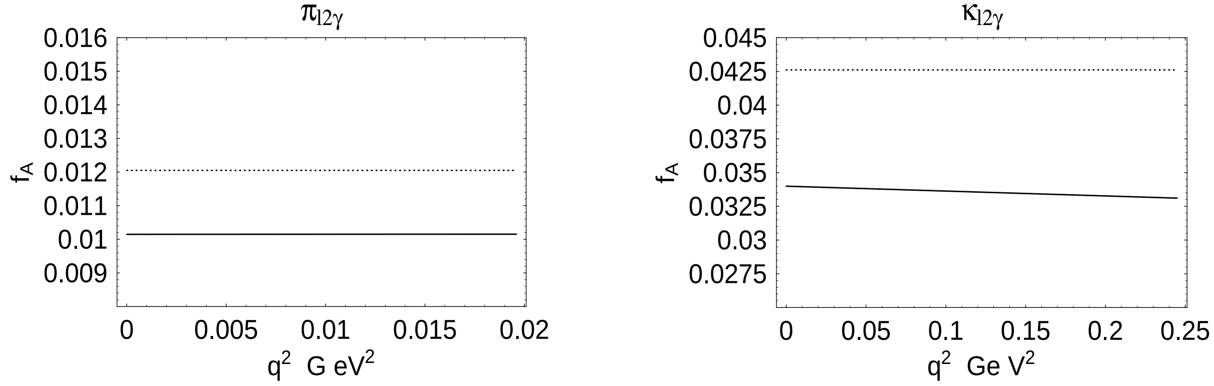

Figure 6: Same as Figure 5 but for the axial-vector form factors f_A. The dashed and solid curves represent the contributions at $O(p^4)$ in Table 3 and the fitting $O(p^4)+O(p^6)$, respectively.

In Figure 5, the dot, solid and dashed curves stand for the contributions to f_V at $O(p^4)$, $O(p^4) + O(p^6)$ in VMD and $O(p^4) + O(p^6)$ in CQM, respectively. We note that for $K_{l2\gamma}$ in Figure 5 F has been set to F_π in Eq. (29) for the curve of $O(p^4)$ as in the literature and F_K in Eq. (32) for those of $O(p^4) + O(p^6)$. As shown in Figure 5, the $O(p^6)$ contribution obtained for the π radiative decays is very small ($< 5\%$) for all the kinematical allowed values. However, it is interesting to see that the $O(p^6)$ correction for $K_{\ell 2\gamma}$ is much larger.

In Figure 6, for f_A, the dashed and solid curves represent the contributions at $O(p^4)$ in Table 3 plus the two-loop calculations using either the LMD or the RL determinations, respectively. It is easy to see that, as shown in the figures, the two-loop contributions to f_A are sizable and destructive compared with those at the pure $O(p^4)$ for both π and K modes, but their q^2-dependences, which are dominated by the irreducible diagrams, are small. At $q^2 = 0$, the contributions to f_A from $f_{A,tree}(p^6)$ are vanishingly small, which implies that the final results of f_A are insensitive to the known values of y_i^r. However, those from the irreducible two-loop diagrams and the one-loop diagrams with one vertex of $\mathcal{L}_n^{(4)}$ give the dominant corrections to f_A at $O(p^4)$. All together the $O(p^6)$ corrections keep around 25% for both decays. We remark that the uncertainties in Eqs. (55) and (56) due to the errors of y_i^r [25] are less than 1%. Moreover, our results of tree contributions at $O(p^6)$ are also insensitive to the choice of the scale, as expected.

We note that, as shown in Figure 5, the numerical result for $\pi \to e\nu_e\gamma$ at $O(p^6)$, using the $SU(3)\otimes SU(3)$ chiral symmetry, is found to be comparable to the one in Ref. [24] from resonance estimates of $O(p^6)$ low-energy constants based on $SU(2)\otimes SU(2)$. Furthermore, our result of the $O(p^6)$ correction for f_A in $K_{l2\gamma}$ also confirms the speculation in Ref. [24].

In summary, we have studied the $O(p^6)$ corrections to the vector and axial-vector form factors in $\pi_{\ell 2\gamma}$ and $K_{\ell 2\gamma}$ decays. These include the contributions from loop diagrams and the ones from higher dimension terms in the lagrangians. The former can be exactly calculated in terms of the known parameters of the chiral lagrangians. The latter is mainly evaluated from the resonance contributions. For the axial-vector form factors of f_A, we have found that the divergent parts cancel order by order in ChPT, while the finite numerical results in both K and π modes contain considerable corrections from loops diagrams; they also agree with the recent experimental determination [37, 38]. This demonstrates numerically the statement about the final-state theorem mentioned in Ref. [19, 20, 21]. Finally, we remark that our result of f_A at q^2=0 for the kaon case is consistent with that found in the light front QCD model [40, 41] as well.

Acknowledgments

We would like to thank Drs. Bijnens and Talavera for encouragement and comments. We would also like to thank Elizabeth Walter for reading the manuscript. This work was supported in part by the National Science Council of the Republic of China under contract numbers NSC-91-2112-M-007-043.

Appendix A

From Figure 3, we have

$$\begin{aligned}
M_{A,\pi,2-point} = {} & \frac{\sqrt{2}eG_F l^\mu \varepsilon^\nu}{12\times 24F^3}\cos\theta[-40\sqrt{2}I(m_K,m_K,m_\pi)+40\sqrt{2}I(m_\pi,m_K,m_K) \\
& +24\sqrt{2}I(m_K,m_K,m_\eta)-24\sqrt{2}I(m_\eta,m_K,m_K)-240\sqrt{2}II(m_K,m_\pi,m_K) \\
& -40\sqrt{2}II(m_\pi,m_K,m_K)-320\sqrt{2}II(m_\pi,m_\pi,m_\pi) \\
& -48\sqrt{2}II(m_K,m_K,m_\eta)-72\sqrt{2}II(m_\eta,m_K,m_K) \\
& +240\sqrt{2}III(m_K,m_K,m_\pi)+40\sqrt{2}III(m_K,m_\pi,m_K) \\
& +320\sqrt{2}III(m_\pi,m_\pi,m_\pi)+96\sqrt{2}III(m_\eta,m_K,m_K) \\
& +72\sqrt{2}III(m_K,m_\eta,m_K)-48\sqrt{2}III(m_K,m_K,m_\eta)], \qquad (58)
\end{aligned}$$

$$\begin{aligned}
M_{A,K,2-point} = {} & \frac{\sqrt{2}eG_F l^\mu \varepsilon^\nu}{12\times 24F^3}\sin\theta[-36\sqrt{2}I(m_\eta,m_\eta,m_K)+36\sqrt{2}I(m_K,m_\eta,m_\eta) \\
& -36\sqrt{2}I(m_\pi,m_\pi,m_K)+36\sqrt{2}I(m_K,m_\pi,m_\pi) \\
& -36\sqrt{2}II(m_K,m_\eta,m_\eta)-336\sqrt{2}II(m_K,m_K,m_K) \\
& -36\sqrt{2}II(m_K,m_\pi,m_\pi)-168\sqrt{2}II(m_\pi,m_\pi,m_K) \\
& -36\sqrt{2}II(m_\eta,m_K,m_\pi)-96\sqrt{2}II(m_K,m_\pi,m_\eta) \\
& -12\sqrt{2}II(m_\pi,m_K,m_\eta)+36\sqrt{2}III(m_\eta,m_K,m_\eta) \\
& +336\sqrt{2}III(m_K,m_K,m_K)+168\sqrt{2}III(m_\pi,m_\pi,m_K) \\
& +36\sqrt{2}III(m_\pi,m_K,m_\pi)-36\sqrt{2}III(m_\pi,m_\eta,m_K) \\
& +72\sqrt{2}III(m_K,m_\eta,m_\pi)+48\sqrt{2}III(m_\eta,m_K,m_\pi) \\
& +48\sqrt{2}III(m_\pi,m_K,m_\eta)+24\sqrt{2}III(m_K,m_\pi,m_\eta) \\
& -12\sqrt{2}III(m_\eta,m_\pi,m_K)]. \qquad (59)
\end{aligned}$$

Form Figure 4, we obtain

$$\begin{aligned}
M_{A,K,3-point} = {} & \frac{i\sqrt{2}}{12F^3}eG_F l^\mu \varepsilon^\nu \sin\theta\{6\sqrt{2}m_K^2 A(m_K,m_K,m_K) \\
& +\sqrt{2}(m_K^2+m_\pi^2)A(m_\pi,m_\pi,m_K)+\frac{\sqrt{2}}{2}(m_K^2+m_\pi^2)A(m_K,m_\pi,m_\pi) \\
& +\frac{\sqrt{2}}{2}(3m_K^2-m_\pi^2)A(m_K,m_\eta,m_\eta)+\frac{\sqrt{2}}{3}(m_K^2-m_\pi^2)A(m_\pi,m_\eta,m_K) \\
& -\frac{\sqrt{2}}{3}(m_K^2-m_\pi^2)A(m_K,m_\eta,m_\pi) \\
& \\
& -\sqrt{2}(m_K^2+m_\pi^2)B(m_\pi,m_\pi,m_K)-6\sqrt{2}m_K^2 B(m_K,m_K,m_K) \\
& -\frac{\sqrt{2}}{2}(m_K^2+m_\pi^2)B(m_\pi,m_K,m_\pi)-\frac{\sqrt{2}}{2}(3m_K^2-m_\pi^2)B(m_\eta,m_K,m_\eta) \\
& +\frac{\sqrt{2}}{6}(m_K^2-m_\pi^2)B(m_\pi,m_K,m_\eta)-\frac{2\sqrt{2}}{3}(m_K^2-m_\pi^2)B(m_K,m_\pi,m_\eta) \\
& +\frac{\sqrt{2}}{6}(m_K^2-m_\pi^2)B(m_\eta,m_K,m_\pi)+\frac{\sqrt{2}}{3}(m_K^2-m_\pi^2)B(m_\eta,m_\pi,m_K)
\end{aligned}$$

$$\begin{gathered}
+\sqrt{2}C(m_K,m_K,m_K)-\frac{\sqrt{2}}{2}C(m_\pi,m_\pi,m_K)-\frac{\sqrt{2}}{2}C(m_K,m_\pi,m_\pi)\\
-\frac{3\sqrt{2}}{2}C(m_K,m_\eta,m_\eta)-\frac{\sqrt{2}}{2}C(m_\pi,m_\eta,m_K)-\sqrt{2}C(m_K,m_\eta,m_\pi)
\end{gathered}$$

$$\begin{gathered}
-7\sqrt{2}D(m_K,m_K,m_K)-\frac{5\sqrt{2}}{2}D(m_\pi,m_\pi,m_K)-\frac{7\sqrt{2}}{4}D(m_\pi,m_K,m_\pi)\\
-\frac{\sqrt{2}}{2}D(m_\eta,m_\pi,m_K)-\frac{\sqrt{2}}{4}D(m_\pi,m_K,m_\eta)-2\sqrt{2}D(m_K,m_\pi,m_\eta)\\
-\frac{\sqrt{2}}{4}D(m_\eta,m_K,m_\pi)-\frac{3\sqrt{2}}{4}D(m_\eta,m_K,m_\eta)
\end{gathered}$$

$$\begin{gathered}
-7\sqrt{2}E(m_K,m_K,m_K)-\frac{5\sqrt{2}}{2}E(m_\pi,m_K,m_\pi)-\frac{7\sqrt{2}}{4}E(m_K,m_\pi,m_\pi)\\
-\frac{\sqrt{2}}{2}E(m_\pi,m_K,m_\eta)-\frac{\sqrt{2}}{4}E(m_K,m_\eta,m_\pi)-\frac{3\sqrt{2}}{4}E(m_K,m_\eta,m_\eta)\\
-\frac{\sqrt{2}}{4}E(m_K,m_\pi,m_\eta)-2\sqrt{2}E(m_\pi,m_\eta,m_K)
\end{gathered}$$

$$\begin{gathered}
+\sqrt{2}F(m_K,m_K,m_K)-\frac{\sqrt{2}}{2}F(m_\pi,m_K,m_\pi)-\frac{\sqrt{2}}{2}F(m_\pi,m_\pi,m_K)\\
-\frac{3\sqrt{2}}{2}F(m_\eta,m_\eta,m_K)-\frac{\sqrt{2}}{2}F(m_\eta,m_K,m_\pi)-\sqrt{2}F(m_\eta,m_\pi,m_K)
\end{gathered}$$

$$\begin{gathered}
-\sqrt{2}G(m_K,m_K,m_K)-\sqrt{2}G(m_\pi,m_K,m_\pi)+\frac{\sqrt{2}}{2}G(m_K,m_\pi,m_\pi)\\
+\frac{3\sqrt{2}}{2}G(m_K,m_\eta,m_\eta)+\frac{\sqrt{2}}{2}G(m_K,m_\eta,m_\pi)+\frac{\sqrt{2}}{2}G(m_K,m_\pi,m_\eta)\\
+\frac{3\sqrt{2}}{2}G(m_\pi,m_\pi,m_K)+\sqrt{2}G(m_\pi,m_K,m_\eta)-\frac{\sqrt{2}}{2}G(m_\pi,m_\eta,m_K)
\end{gathered}$$

$$\begin{gathered}
-\sqrt{2}H(m_K,m_K,m_K)+\frac{3\sqrt{2}}{2}H(m_\pi,m_\pi,m_K)-\sqrt{2}H(m_K,m_\pi,m_\pi)\\
+\frac{\sqrt{2}}{2}H(m_\pi,m_K,m_\pi)+\sqrt{2}H(m_K,m_\pi,m_\eta)+\frac{\sqrt{2}}{2}H(m_\pi,m_K,m_\eta)\\
+\frac{3\sqrt{2}}{2}H(m_\eta,m_K,m_\eta)+\frac{\sqrt{2}}{2}H(m_\eta,m_K,m_\pi)-\frac{\sqrt{2}}{2}H(m_\eta,m_\pi,m_K)
\end{gathered}$$

$$\begin{gathered}
+8\sqrt{2}I(m_K,m_K,m_K)+\sqrt{2}I(m_K,m_\pi,m_\pi)+\sqrt{2}I(m_\pi,m_K,m_\pi)\\
+\frac{5\sqrt{2}}{4}I(m_\pi,m_\pi,m_K)-\frac{3\sqrt{2}}{4}I(m_\eta,m_\eta,m_K)+\sqrt{2}I(m_K,m_\eta,m_\pi)\\
+\sqrt{2}I(m_\eta,m_K,m_\pi)-\frac{\sqrt{2}}{4}I(m_\pi,m_\eta,m_K)-\frac{\sqrt{2}}{4}I(m_\eta,m_\pi,m_K)
\end{gathered}$$

$$
\begin{aligned}
&-\sqrt{2}J(m_K,m_K,m_K)-\sqrt{2}J(m_\pi,m_\pi,m_K)+\frac{\sqrt{2}}{2}J(m_K,m_\pi,m_\pi)\\
&-\frac{\sqrt{2}}{2}J(m_\pi,m_K,m_\eta)+\frac{3\sqrt{2}}{2}J(m_\pi,m_K,m_\pi)+\frac{\sqrt{2}}{2}J(m_K,m_\pi,m_\eta)\\
&+\frac{\sqrt{2}}{2}J(m_K,m_\eta,m_\pi)+\frac{3\sqrt{2}}{2}J(m_K,m_\eta,m_\eta)+\sqrt{2}J(m_\pi,m_\eta,m_K)\\
&\\
&+8\sqrt{2}K(m_K,m_K,m_K)+\sqrt{2}K(m_K,m_\pi,m_\pi)+\sqrt{2}K(m_\pi,m_\pi,m_K)\\
&+\frac{5\sqrt{2}}{4}K(m_\pi,m_K,m_\pi)-\frac{3\sqrt{2}}{4}K(m_\eta,m_K,m_\eta)-\frac{\sqrt{2}}{4}K(m_\pi,m_K,m_\eta)\\
&-\frac{\sqrt{2}}{4}K(m_\eta,m_K,m_\pi)+\sqrt{2}K(m_\eta,m_\pi,m_K)+\sqrt{2}K(m_K,m_\pi,m_\eta)\\
&\\
&-\sqrt{2}L(m_K,m_K,m_K)-\sqrt{2}L(m_K,m_\pi,m_\pi)+\frac{\sqrt{2}}{2}L(m_\pi,m_\pi,m_K)\\
&+\frac{3\sqrt{2}}{2}L(m_\eta,m_\eta,m_K)+\frac{\sqrt{2}}{2}L(m_\eta,m_\pi,m_K)+\sqrt{2}L(m_K,m_\eta,m_\pi)\\
&+\frac{3\sqrt{2}}{2}L(m_\pi,m_K,m_\pi)+\frac{\sqrt{2}}{2}L(m_\pi,m_\eta,m_K)-\frac{\sqrt{2}}{2}L(m_\eta,m_K,m_\pi)\}
\end{aligned}
\tag{60}
$$

$$
\begin{aligned}
M_{A,\pi,3-point} &= \frac{i\sqrt{2}}{12F^3}eG_F l^\mu\varepsilon^\nu\cos\theta\{\sqrt{2}(m_K^2+m_\pi^2)A(m_K,m_\pi,m_K)\\
&+\frac{20\sqrt{2}}{3}m_\pi^2A(m_\pi,m_\pi,m_\pi)+\frac{2\sqrt{2}}{3}(m_K^2+m_\pi^2)A(m_\pi,m_K,m_K)\\
&-\frac{\sqrt{2}}{3}(m_\pi^2-m_K^2)A(m_K,m_K,m_\eta)\\
&\\
&-\sqrt{2}(m_K^2+m_\pi^2)B(m_K,m_K,m_\pi)-\frac{2\sqrt{2}}{3}(m_K^2+m_\pi^2)B(m_K,m_\pi,m_K)\\
&-\frac{20\sqrt{2}}{3}m_\pi^2B(m_\pi,m_\pi,m_\pi)+\frac{2\sqrt{2}}{3}(m_\pi^2-m_K^2)B(m_\eta,m_K,m_K)\\
&-\frac{\sqrt{2}}{3}(m_\pi^2-m_K^2)B(m_K,m_K,m_\eta)\\
&\\
&+\sqrt{2}C(m_K,m_\pi,m_K)-\frac{4\sqrt{2}}{3}C(m_\pi,m_\pi,m_\pi)-\frac{2\sqrt{2}}{3}C(m_\pi,m_K,m_K)\\
&-\frac{3\sqrt{2}}{2}C(m_K,m_K,m_\pi)-\frac{\sqrt{2}}{2}C(m_K,m_K,m_\eta)\\
&\\
&-\frac{5\sqrt{2}}{2}D(m_K,m_K,m_\pi)-\frac{20\sqrt{2}}{3}D(m_\pi,m_\pi,m_\pi)\\
&-\frac{10\sqrt{2}}{3}D(m_K,m_\pi,m_K)-\frac{\sqrt{2}}{2}D(m_K,m_K,m_\eta)-2\sqrt{2}D(m_\eta,m_K,m_K)
\end{aligned}
$$

$$
\begin{aligned}
&-\frac{5\sqrt{2}}{2}E(m_K,m_\pi,m_K)-\frac{20\sqrt{2}}{3}E(m_\pi,m_\pi,m_\pi)\\
&-\frac{10\sqrt{2}}{3}E(m_\pi,m_K,m_K)-2\sqrt{2}E(m_K,m_K,m_\eta)-\frac{\sqrt{2}}{2}E(m_K,m_\eta,m_K)\\
&-\frac{\sqrt{2}}{2}F(m_\pi,m_K,m_K)-\frac{4\sqrt{2}}{3}F(m_\pi,m_\pi,m_\pi)-\frac{2\sqrt{2}}{3}F(m_K,m_K,m_\pi)\\
&-\frac{\sqrt{2}}{2}F(m_\eta,m_K,m_K)\\
&-\sqrt{2}G(m_K,m_\pi,m_K)+\frac{4\sqrt{2}}{3}G(m_\pi,m_\pi,m_\pi)+\frac{2\sqrt{2}}{3}G(m_\pi,m_K,m_K)\\
&+\frac{3\sqrt{2}}{2}G(m_K,m_K,m_\pi)-\frac{\sqrt{2}}{2}G(m_K,m_K,m_\eta)+\sqrt{2}G(m_K,m_\eta,m_K)\\
&-\sqrt{2}H(m_\pi,m_K,m_K)+\frac{2\sqrt{2}}{3}H(m_K,m_\pi,m_K)+\frac{4\sqrt{2}}{3}H(m_\pi,m_\pi,m_\pi)\\
&+\frac{3\sqrt{2}}{2}H(m_K,m_K,m_\pi)+\sqrt{2}H(m_\eta,m_K,m_K)-\frac{\sqrt{2}}{2}H(m_K,m_K,m_\eta)\\
&+\sqrt{2}I(m_\pi,m_K,m_K)+\sqrt{2}I(m_K,m_\pi,m_K)+\frac{16\sqrt{2}}{3}I(m_\pi,m_\pi,m_\pi)\\
&+\frac{8\sqrt{2}}{3}I(m_K,m_K,m_\pi)+\sqrt{2}I(m_K,m_\eta,m_K)+\sqrt{2}I(m_\eta,m_K,m_K)\\
&-\sqrt{2}J(m_K,m_K,m_\pi)+\frac{4\sqrt{2}}{3}J(m_\pi,m_\pi,m_\pi)+\frac{2\sqrt{2}}{3}J(m_\pi,m_K,m_K)\\
&+\frac{3\sqrt{2}}{2}J(m_K,m_\pi,m_K)+\sqrt{2}J(m_K,m_K,m_\eta)-\frac{\sqrt{2}}{2}J(m_K,m_\eta,m_K)\\
&+\sqrt{2}K(m_K,m_K,m_\pi)+\sqrt{2}K(m_\pi,m_K,m_K)+\frac{16\sqrt{2}}{3}K(m_\pi,m_\pi,m_\pi)\\
&+\frac{8\sqrt{2}}{3}K(m_K,m_\pi,m_K)+\sqrt{2}K(m_\eta,m_K,m_K)+\sqrt{2}K(m_K,m_K,m_\eta)\\
&-\sqrt{2}L(m_\pi,m_K,m_K)+\frac{4\sqrt{2}}{3}L(m_\pi,m_\pi,m_\pi)+\frac{2\sqrt{2}}{3}L(m_K,m_K,m_\pi)\\
&+\frac{3\sqrt{2}}{2}L(m_K,m_\pi,m_K)-\frac{\sqrt{2}}{2}L(m_K,m_\eta,m_K)+\sqrt{2}L(m_\eta,m_K,m_K)\Big\}
\end{aligned}
\tag{61}
$$

Appendix B

We list the functions $\{II, III, \cdots, A, B, \cdots, L\}$ in Figures 3 and 4 by scalar integrals of $P^{ab}_{\alpha1,\alpha2,\alpha3}$ and one-loop tadpole integrals T_1, T_2 in the Euclidian space. We note that the function I does not contain $g^{\mu\nu}$ and thus it has no contribution to F_A. For simplicity, we only give the formulas related to terms with $g_{\mu\nu}$ due to the definition of F_A. We have

$$\begin{aligned} II(m_1, m_2, m_3) &= \frac{-ig^{\mu\nu}}{(2\pi)^{2n}(n-1)}\Big[T_1(m_2^2)T_1(m_3^2) - m_1^2 P^{00}_{111}(m_1, m_2, m_3) \\ &\quad -\frac{1}{\ell^2}P^{20}_{111}(m_1, m_2, m_3)\Big] + \cdots , \end{aligned} \tag{62}$$

$$\begin{aligned} III(m_1, m_2, m_3) &= \frac{-ig^{\mu\nu}}{(2\pi)^{2n}(n-1)}\Big[\frac{1}{2}T_1(m_1^2)T_1(m_2^2) - \frac{1}{2}T_1(m_2^2)T_1(m_3^2) - \frac{1}{2}T_1(m_1^2)T_1(m_3^2) \\ &\quad +\frac{1}{2}(m_1^2 + m_2^2 - m_3^2 - \ell^2)P^{00}_{111}(m_1, m_2, m_3) - P^{10}_{111}(m_1, m_2, m_3) \\ &\quad -P^{01}_{111}(m_1, m_2, m_3) - \frac{1}{\ell^2}P^{11}_{111}(m_1, m_2, m_3)\Big] + \cdots , \end{aligned} \tag{63}$$

$$\begin{aligned} A(m_1, m_2, m_3) &= \frac{-2g^{\mu\nu}}{(2\pi)^{2n}(n-1)}\int dx(-1)\Big[P^{00}_{111}(m_1, m_2, m_3) - m_1^2 P^{00}_{211}(m_1, m_2, m_3) \\ &\quad -\frac{1}{\ell'^2}P^{20}_{211}(m_1, m_2, m_3)\Big] + \cdots , \end{aligned} \tag{64}$$

$$\begin{aligned} B(m_1, m_2, m_3) &= \frac{-g^{\mu\nu}}{(2\pi)^{2n}(n-1)}\int dx(-1)\Big[T_2(m_2^2)T_1(m_1^2) - T_2(m_2^2)T_1(m_3^2) \\ &\quad -P^{00}_{111}(m_2, m_1, m_3) + (m_1^2 + m_2^2 - m_3^2 - \ell'^2)P^{00}_{211}(m_2, m_1, m_3) \\ &\quad -2P^{10}_{211}(m_2, m_1, m_3) - 2P^{01}_{211}(m_2, m_1, m_3) \\ &\quad -\frac{2}{\ell'^2}P^{11}_{211}(m_2, m_1, m_3)\Big] + \cdots , \end{aligned} \tag{65}$$

$$\begin{aligned} & C(m_1, m_2, m_3) + F(m_3, m_1, m_2) \\ = \; & \frac{g^{\mu\nu}}{(2\pi)^{2n}(n-1)}\int dx\Big[2(1-x)(p_M\cdot k)P^{00}_{111}(m_1, m_2, m_3) \\ & -\frac{2(p_M\cdot\ell')}{\ell'^2}P^{10}_{111}(m_1, m_2, m_3) - T_1(m_1^2)T_1(m_2^2) + T_1(m_2^2)T_1(m_3^2) - T_1(m_1^2)T_1(m_3^2) \\ & +2P^{10}_{111}(m_1, m_2, m_3) + (-m_1^2 + m_2^2 + m_3^2 + \ell'^2)P^{00}_{111}(m_1, m_2, m_3) \\ & -2m_1^2(1-x)(p_M\cdot k)P^{00}_{211}(m_1, m_2, m_3) + 2m_1^2\frac{(p_M\cdot\ell')}{\ell'^2}P^{10}_{211}(m_1, m_2, m_3) \\ & +m_1^2 T_2(m_1^2)T_1(m_2^2) - m_1^2 P^{00}_{111}(m_1, m_2, m_3) + m_1^2 T_2(m_1^2)T_1(m_3^2) \\ & -2m_1^2 P^{10}_{211}(m_1, m_2, m_3) - m_1^2(-m_1^2 + m_2^2 + m_3^2 + \ell'^2)P^{00}_{211}(m_1, m_2, m_3) \\ & -\frac{2(1-x)(p_M\cdot k)}{\ell'^2}P^{20}_{211}(m_1, m_2, m_3) + \frac{2(p_M\cdot\ell')}{\ell'^4}P^{30}_{211}(m_1, m_2, m_3) \\ & -\frac{2}{\ell'^2}P^{30}_{211}(m_1, m_2, m_3) - \frac{1}{\ell'^2}(-m_1^2 + m_2^2 + m_3^2 + \ell'^2)P^{20}_{211}(m_1, m_2, m_3) \\ & +\frac{1}{\ell'^2}T_1(m_2^2)\int\frac{d^n p(p\cdot\ell')^2}{(p^2 + m_1^2)^2} - \frac{1}{\ell'^2}P^{20}_{111}(m_1, m_2, m_3) \end{aligned}$$

$$
+\frac{1}{\ell'^2}T_1(m_3^2)\int\frac{d^np(p\cdot\ell')^2}{(p^2+m_1^2)^2}\Bigg]+\cdots, \tag{66}
$$

$$
\begin{aligned}
& D(m_2,m_1,m_3)+E(m_1,m_3,m_2)\\
= & \frac{-g^{\mu\nu}}{(2\pi)^{2n}(n-1)}\int dx\Bigg\{T_1(m_1^2)\int d^np\frac{p^2}{(p^2+m_2^2)^2}-(1-x)(\ell'\cdot k)T_2(m_2^2)T_1(m_1^2)\\
& -\frac{(p_M\cdot\ell')}{\ell'^2}P^{01}_{111}(m_2,m_1,m_3)+(1-x)(\ell'\cdot k)P^{00}_{111}(m_2,m_1,m_3)\\
& +\frac{(1-x)(\ell'\cdot k)}{\ell'^2}P^{01}_{111}(m_2,m_1,m_3)+\frac{(1-x)(\ell'\cdot k)}{\ell'^2}P^{10}_{111}(m_2,m_1,m_3)\\
& -\frac{1}{2}T_1(m_1^2)T_1(m_3^2)+\frac{1}{2}m_2^2P^{00}_{111}(m_2,m_1,m_3)-\frac{1}{2}T_1(m_2^2)T_1(m_1^2)+\frac{1}{2}T_1(m_2^2)T_1(m_3^2)\\
& -\frac{1}{2}(m_1^2-\ell'^2-m_3^2)P^{00}_{111}(m_2,m_1,m_3)+P^{01}_{111}(m_2,m_1,m_3)+(p_M\cdot\ell')T_2(m_2^2)T_1(m_3^2)\\
& +(m_1^2+m_2^2-\ell'^2-m_3^2)\Bigg[\frac{(p_M\cdot\ell')}{\ell'^2}P^{01}_{211}(m_2,m_1,m_3)-(1-x)(\ell'\cdot k)P^{00}_{211}(m_2,m_1,m_3)\\
& -\frac{(1-x)(\ell'\cdot k)}{\ell'^2}P^{01}_{211}(m_2,m_1,m_3)-\frac{(1-x)(\ell'\cdot k)}{\ell'^2}P^{10}_{211}(m_2,m_1,m_3)\\
& +\frac{1}{2}P^{00}_{111}(m_2,m_1,m_3)-\frac{1}{2}m_2^2P^{00}_{211}(m_2,m_1,m_3)+\frac{1}{2}T_2(m_2^2)T_1(m_1^2)-\frac{1}{2}T_2(m_2^2)T_1(m_3^2)\\
& +\frac{1}{2}(m_1^2-\ell'^2-m_3^2)P^{00}_{211}(m_2,m_1,m_3)-P^{01}_{211}(m_2,m_1,m_3)\Bigg]\\
& -2\frac{(p_M\cdot\ell')}{\ell'^2}P^{02}_{211}(m_2,m_1,m_3)+2(1-x)(\ell'\cdot k)P^{01}_{211}(m_2,m_1,m_3)\\
& +\frac{2(1-x)(\ell'\cdot k)}{\ell'^2}P^{02}_{211}(m_2,m_1,m_3)+\frac{2(1-x)(\ell'\cdot k)}{\ell'^2}P^{11}_{211}(m_2,m_1,m_3)\\
& -P^{01}_{111}(m_2,m_1,m_3)+m_2^2P^{01}_{211}(m_2,m_1,m_3)-\ell'^2T_2(m_2^2)T_1(m_3^2)\\
& -(m_1^2-\ell'^2-m_3^2)P^{01}_{211}(m_2,m_1,m_3)+2P^{02}_{211}(m_2,m_1,m_3)\\
& -2\frac{(p_M\cdot\ell')}{\ell'^2}P^{11}_{211}(m_2,m_1,m_3)+2(1-x)(\ell'\cdot k)P^{10}_{211}(m_2,m_1,m_3)\\
& +\frac{2(1-x)(\ell'\cdot k)}{\ell'^2}P^{11}_{211}(m_2,m_1,m_3)+\frac{2(1-x)(\ell'\cdot k)}{\ell'^2}P^{20}_{211}(m_2,m_1,m_3)\\
& -P^{10}_{111}(m_2,m_1,m_3)+m_2^2P^{10}_{211}(m_2,m_1,m_3)-(m_1^2-\ell'^2-m_3^2)P^{10}_{211}(m_2,m_1,m_3)\\
& +2P^{11}_{211}(m_2,m_1,m_3)-\frac{2(p_M\cdot\ell')}{\ell'^4}P^{12}_{211}(m_2,m_1,m_3)\\
& +\frac{2(1-x)(\ell'\cdot k)}{\ell'^2}P^{11}_{211}(m_2,m_1,m_3)+2\frac{(1-x)(\ell'\cdot k)}{\ell'^4}P^{12}_{211}(m_2,m_1,m_3)\\
& +\frac{2(1-x)(\ell'\cdot k)}{\ell'^4}P^{21}_{211}(m_2,m_1,m_3)-\frac{1}{\ell'^2}P^{11}_{111}(m_2,m_1,m_3)\\
& +\frac{1}{\ell'^2}m_2^2P^{11}_{211}(m_2,m_1,m_3)-\frac{(m_1^2-\ell'^2-m_3^2)}{\ell'^2}P^{11}_{211}(m_2,m_1,m_3)\\
& +\frac{2}{\ell'^2}P^{12}_{211}(m_2,m_1,m_3)-\frac{1}{\ell'^2}T_1(m_3^2)\int\frac{d^np(p\cdot\ell')^2}{(p^2+m_2^2)^2}\Bigg\}+\cdots,
\end{aligned}
\tag{67}
$$

$$
H(m_2,m_1,m_3)+J(m_1,m_3,m_2)
$$

$$
\begin{aligned}
= \;& \frac{-g^{\mu\nu}}{(2\pi)^{2n}(n-1)}\int dx\,\Big\{\frac{2(p_M\cdot\ell')}{\ell'^2}P^{01}_{111}(m_2,m_1,m_3)+2P^{10}_{111}(m_2,m_1,m_3)\\
&-2(1-x)(\ell'\cdot k)P^{00}_{111}(m_2,m_1,m_3)-\frac{2(1-x)(\ell'\cdot k)}{\ell'^2}P^{10}_{111}(m_2,m_1,m_3)\\
&-\frac{2(1-x)(\ell'\cdot k)}{\ell'^2}P^{01}_{111}(m_2,m_1,m_3)+T_1(m_2^2)T_1(m_1^2)\\
&+(-m_2^2+m_1^2-\ell'^2-m_3^2)P^{00}_{111}(m_2,m_1,m_3)-2P^{10}_{111}(m_2,m_1,m_3)\\
&-2P^{01}_{111}(m_2,m_1,m_3)+T_1(m_1^2)T_1(m_3^2)-T_1(m_2^2)T_1(m_3^2)\\
&-\frac{2m_2^2(p_M\cdot\ell')}{\ell'^2}P^{01}_{211}(m_2,m_1,m_3)-2m_2^2P^{10}_{211}(m_2,m_1,m_3)\\
&+2m_2^2(1-x)(\ell'\cdot k)P^{00}_{211}(m_2,m_1,m_3)+\frac{2m_2^2(1-x)(\ell'\cdot k)}{\ell'^2}P^{10}_{211}(m_2,m_1,m_3)\\
&+\frac{2m_2^2(1-x)(\ell'\cdot k)}{\ell'^2}P^{01}_{211}(m_2,m_1,m_3)-m_2^2T_1(m_2^2)T_1(m_1^2)\\
&-m_2^2(-m_2^2+m_1^2-\ell'^2-m_3^2)P^{00}_{211}(m_2,m_1,m_3)+2m_2^2P^{10}_{211}(m_2,m_1,m_3)\\
&+2m_2^2P^{01}_{211}(m_2,m_1,m_3)+m_2^2T_2(m_2^2)T_1(m_3^2)-m_2^2P^{00}_{111}(m_2,m_1,m_3)\\
&-\frac{2(p_M\cdot\ell')}{\ell'^4}P^{21}_{211}(m_2,m_1,m_3)-\frac{2}{\ell'^2}P^{30}_{211}(m_2,m_1,m_3)\\
&+\frac{2(1-x)(\ell'\cdot k)}{\ell'^2}P^{20}_{211}(m_2,m_1,m_3)+2\frac{(1-x)(\ell'\cdot k)}{\ell'^4}P^{30}_{211}(m_2,m_1,m_3)\\
&+\frac{2(1-x)(\ell'\cdot k)}{\ell'^4}P^{21}_{211}(m_2,m_1,m_3)-T_1(m_1^2)\int\frac{d^np\frac{(p\cdot\ell')^2}{\ell'^2}}{(p^2+m_2^2)^2}\\
&-\frac{(-m_2^2+m_1^2-\ell'^2-m_3^2)}{\ell'^2}P^{20}_{211}(m_2,m_1,m_3)+\frac{2}{\ell'^2}P^{30}_{211}(m_2,m_1,m_3)\\
&+\frac{2}{\ell'^2}P^{21}_{211}(m_2,m_1,m_3)-\frac{1}{\ell'^2}P^{20}_{111}(m_2,m_1,m_3)+T_1(m_3^2)\int\frac{d^np\frac{(p\cdot\ell')^2}{\ell'^2}}{(p^2+m_2^2)^2}\Big\}\\
&+\cdots,
\end{aligned}
\tag{68}
$$

$$
\begin{aligned}
&I(m_3,m_2,m_1)+K(m_2,m_1,m_3)\\
= \;& \frac{g^{\mu\nu}}{(2\pi)^{2n}(n-1)}\int dx\,\Big\{(p_M\cdot\ell')T_2(m_3^2)T_1(m_2^2)\\
&-(p_M\cdot\ell')P^{00}_{111}(m_3,m_2,m_1)-\frac{(p_M\cdot\ell')}{\ell'^2}P^{10}_{111}(m_3,m_2,m_1)\\
&-\frac{(p_M\cdot\ell')}{\ell'^2}P^{01}_{111}(m_3,m_2,m_1)+\frac{(1-x)(\ell'\cdot k)}{\ell'^2}P^{01}_{111}(m_3,m_2,m_1)\\
&-\frac{1}{2}T_1(m_3^2)T_1(m_2^2)+\frac{1}{2}T_1(m_2^2)T_1(m_1^2)+\frac{1}{2}T_1(m_3^2)T_1(m_1^2)\\
&-\frac{1}{2}(m_2^2-m_1^2-\ell'^2+m_3^2)P^{00}_{111}(m_3,m_2,m_1)+P^{10}_{111}(m_3,m_2,m_1)\\
&+P^{01}_{111}(m_3,m_2,m_1)-(1-x)(\ell'\cdot k)T_2(m_3^2)T_1(m_1^2)+T_1(m_1^2)\int\frac{d^np(p)^2}{(p^2+m_3^2)^2}\\
&+(m_3^2+m_2^2-\ell'^2-m_1^2)\times[(p_M\cdot\ell')P^{00}_{211}(m_3,m_2,m_1)\\
&+\frac{(p_M\cdot\ell')}{\ell'^2}P^{10}_{211}(m_3,m_2,m_1)+\frac{(p_M\cdot\ell')}{\ell'^2}P^{01}_{211}(m_3,m_2,m_1)
\end{aligned}
$$

$$
\begin{aligned}
& -\frac{(1-x)(\ell'\cdot k)}{\ell'^2}P^{01}_{211}(m_3,m_2,m_1)+\frac{1}{2}T_2(m_3^2)T_1(m_2^2)-\frac{1}{2}P^{00}_{111}(m_3,m_2,m_1) \\
& -\frac{1}{2}T_2(m_3^2)T_1(m_1^2)+\frac{1}{2}(m_3^2+m_2^2-\ell'^2-m_1^2)P^{00}_{211}(m_3,m_2,m_1) \\
& -P^{10}_{211}(m_3,m_2,m_1)-P^{01}_{211}(m_3,m_2,m_1)] \\
& -2(p_M\cdot\ell')P^{10}_{211}(m_3,m_2,m_1)-\frac{2(p_M\cdot\ell')}{\ell'^2}P^{20}_{211}(m_3,m_2,m_1) \\
& -\frac{2(p_M\cdot\ell')}{\ell'^2}P^{11}_{211}(m_3,m_2,m_1)+2\frac{(1-x)(\ell'\cdot k)}{\ell'^2}P^{11}_{211}(m_3,m_2,m_1) \\
& +P^{10}_{111}(m_3,m_2,m_1)-(m_3^2+m_2^2-\ell'^2-m_1^2)P^{10}_{211}(m_3,m_2,m_1)+2P^{20}_{211}(m_3,m_2,m_1) \\
& +2P^{11}_{211}(m_3,m_2,m_1)-2(p_M\cdot\ell')P^{01}_{211}(m_3,m_2,m_1)-\frac{2(p_M\cdot\ell')}{\ell'^2}P^{11}_{211}(m_3,m_2,m_1) \\
& -\frac{2(p_M\cdot\ell')}{\ell'^2}P^{02}_{211}(m_3,m_2,m_1)+2\frac{(1-x)(\ell'\cdot k)}{\ell'^2}P^{02}_{211}(m_3,m_2,m_1)+P^{01}_{111}(m_3,m_2,m_1) \\
& -\ell'^2T_2(m_3^2)T_1(m_1^2)-(m_3^2+m_2^2-\ell'^2-m_1^2)P^{01}_{211}(m_3,m_2,m_1) \\
& +2P^{11}_{211}(m_3,m_2,m_1)+2P^{02}_{211}(m_3,m_2,m_1)-\frac{2(p_M\cdot\ell')}{\ell'^2}P^{11}_{211}(m_3,m_2,m_1) \\
& -2\frac{(p_M\cdot\ell')}{\ell'^4}P^{21}_{211}(m_3,m_2,m_1)-2\frac{(p_M\cdot\ell')}{\ell'^4}P^{12}_{211}(m_3,m_2,m_1) \\
& +2\frac{(1-x)(\ell'\cdot k)}{\ell'^4}P^{12}_{211}(m_3,m_2,m_1)+\frac{1}{\ell'^2}P^{11}_{111}(m_3,m_2,m_1) \\
& -\frac{(m_3^2+m_2^2-\ell'^2-m_1^2)}{\ell'^2}P^{11}_{211}(m_3,m_2,m_1)+\frac{2}{\ell'^2}P^{21}_{211}(m_3,m_2,m_1) \\
& +\frac{2}{\ell'^2}P^{12}_{211}(m_3,m_2,m_1)-\frac{1}{\ell'^2}T_1(m_1^2)\int\frac{d^np(p\cdot\ell')^2}{(p^2+m_3^2)^2}\Bigg\}+\cdots, \qquad (69)
\end{aligned}
$$

$$
\begin{aligned}
& G(m_1,m_2,m_3)+L(m_3,m_1,m_2) \\
= & \frac{g^{\mu\nu}}{(2\pi)^{2n}(n-1)}\int dx\Bigg\{(p_M\cdot k)(1-x)T_2(m_1^2)T_1(m_2^2)-T_2(m_1^2)\int\frac{d^np\,p^2}{(p^2+m_2^2)} \\
& +\frac{(p_M\cdot\ell')}{\ell'^2}P^{10}_{111}(m_1,m_2,m_3)-(p_M\cdot k)(1-x)P^{00}_{111}(m_1,m_2,m_3) \\
& +P^{01}_{111}(m_1,m_2,m_3)+\frac{1}{2}T_1(m_1^2)T_1(m_2^2)-\frac{1}{2}T_1(m_2^2)T_1(m_3^2)+\frac{1}{2}T_1(m_1^2)T_1(m_3^2) \\
& +\frac{1}{2}(m_1^2-m_2^2-\ell'^2-m_3^2)P^{00}_{111}(m_1,m_2,m_3)-P^{10}_{111}(m_1,m_2,m_3) \\
& -P^{01}_{111}(m_1,m_2,m_3)-(1-x)(p_M\cdot k)T_2(m_1^2)T_1(m_3^2)-(m_1^2+m_2^2-\ell'^2-m_3^2)\times \\
& [\frac{(p_M\cdot\ell')}{\ell'^2}P^{10}_{211}(m_1,m_2,m_3)-(p_M\cdot k)(1-x)P^{00}_{211}(m_1,m_2,m_3) \\
& +P^{01}_{211}(m_1,m_2,m_3)+\frac{1}{2}T_2(m_1^2)T_1(m_2^2)-\frac{1}{2}P^{00}_{111}(m_1,m_2,m_3)+\frac{1}{2}T_2(m_1^2)T_1(m_3^2) \\
& +\frac{1}{2}(m_1^2-m_2^2-\ell'^2-m_3^2)P^{00}_{211}(m_1,m_2,m_3)-P^{10}_{211}(m_1,m_2,m_3) \\
& -P^{01}_{211}(m_1,m_2,m_3)]+2\frac{(p_M\cdot\ell')}{\ell'^2}P^{20}_{211}(m_1,m_2,m_3) \\
& -2(p_M\cdot k)(1-x)P^{10}_{211}(m_1,m_2,m_3)+2P^{11}_{211}(m_1,m_2,m_3) \\
& -P^{10}_{111}(m_1,m_2,m_3)+(m_1^2-m_2^2-\ell'^2-m_3^2)P^{10}_{211}(m_1,m_2,m_3)
\end{aligned}
$$

$$
\begin{aligned}
&-2P^{20}_{211}(m_1,m_2,m_3)-2P^{11}_{211}(m_1,m_2,m_3)\\
&+2\frac{(p_M\cdot\ell')}{\ell'^2}P^{11}_{211}(m_1,m_2,m_3)-2(p_M\cdot k)(1-x)P^{01}_{211}(m_1,m_2,m_3)\\
&+2P^{02}_{211}(m_1,m_2,m_3)-P^{01}_{111}(m_1,m_2,m_3)-\ell'^2T_2(m_1^2)T_1(m_3^2)\\
&+(m_1^2-m_2^2-\ell'^2-m_3^2)P^{01}_{211}(m_1,m_2,m_3)-2P^{11}_{211}(m_1,m_2,m_3)-2P^{02}_{211}(m_1,m_2,m_3)\\
&+\frac{2(p_M\cdot\ell')}{\ell'^4}P^{21}_{211}(m_1,m_2,m_3)-2\frac{(p_M\cdot k)(1-x)}{\ell'^2}P^{11}_{211}(m_1,m_2,m_3)\\
&+\frac{2}{\ell'^2}P^{12}_{211}(m_1,m_2,m_3)-\frac{1}{\ell'^2}P^{11}_{111}(m_1,m_2,m_3)\\
&+\frac{(m_1^2-m_2^2-\ell'^2-m_3^2)}{\ell'^2}P^{11}_{211}(m_1,m_2,m_3)-\frac{2}{\ell'^2}P^{21}_{211}(m_1,m_2,m_3)\\
&\left.-\frac{2}{\ell'^2}P^{12}_{211}(m_1,m_2,m_3)-\frac{1}{\ell'^2}T_1(m_3^2)\int\frac{d^np(p\cdot\ell')^2}{(p^2+m_1^2)^2}\right\}+\cdots,
\end{aligned}
\tag{70}
$$

where $\ell'=\ell+kx$, $n=4-2\epsilon$, P_M represents the meson momentum, and $\{\cdots\}$ correspond to the terms without $g^{\mu\nu}$.

Appendix C

In this Appendix, we will replace the set of ten functions $P_{211}^{ab}(m_1, m_2, m_3; \ell^2)$ by the following equivalent one of $H_i(m_1, m_2, m_3; \ell^2)$ [17]. The functions H_i are free of quadratic divergencies and for this reason they have simpler integral representations.

For the well known one-loop integrals with the definition $\gamma_s = \gamma - 1 - \ln(4\pi)$, we have

$$\begin{aligned}
I(m^2) &\equiv \mu^{4-D} \int \frac{d^D q}{(2\pi)^D} \frac{i}{q^2 - m^2} \\
&= \frac{m^2}{16\pi^2} \left(\frac{m^2}{4\pi\mu^2} \right)^{-\epsilon} \Gamma(-1+\epsilon) \\
&= \frac{-m^2}{16\pi^2} \left\{ \frac{1}{\varepsilon} - \gamma_s - \ln\left(\frac{m^2}{\mu^2}\right) + \epsilon \left[\frac{\pi^2}{12} - \gamma_s - \ln\left(\frac{m^2}{\mu^2}\right) + \frac{1}{2}\left(\gamma_s + 1 + \ln\left(\frac{m^2}{\mu^2}\right)\right)^2 \right] \right\}, \qquad (71)
\end{aligned}$$

$$\begin{aligned}
(2\pi)^{4-n} T_1(m^2) &= (2\pi\mu)^{4-n} \int d^n p \frac{1}{p^2 + m^2} \\
= -m^2\pi^2 &\left\{ \frac{1}{\epsilon} - \gamma_s - \ln\left(\frac{m^2}{\mu^2}\right) + \epsilon \left[\frac{\pi^2}{12} - \gamma_s - \ln\left(\frac{m^2}{\mu^2}\right) + \frac{1}{2}\left(\gamma_s + 1 + \ln\left(\frac{m^2}{\mu^2}\right)\right)^2 \right] \right\}, \qquad (72)
\end{aligned}$$

$$\begin{aligned}
(2\pi)^{4-n} T_2(m^2) &= (2\pi\mu)^{4-n} \int d^n p \frac{1}{(p^2 + m^2)^2} \\
&= \pi^2 \left\{ \frac{1}{\epsilon} - 1 - \gamma_s - \ln\left(\frac{m^2}{\mu^2}\right) + \epsilon \left[\frac{\pi^2}{12} + \frac{1}{2} + \gamma_s + \frac{\gamma_s^2}{2} + \ln\left(\frac{m^2}{\mu^2}\right) + \gamma_s \ln\left(\frac{m^2}{\mu^2}\right) \right.\right. \\
&\qquad \left.\left. + \frac{1}{2} \ln\left(\frac{m^2}{\mu^2}\right) \times \ln\left(\frac{m^2}{\mu^2}\right) \right] \right\} . \qquad (73)
\end{aligned}$$

We note that the expressions of Eq. (71) and Eqs. (72) and (73) are defined in Minkowski and Euclidian spaces, respectively.

For the two-point functions, the relations between P_{111}^{ab} and H_i are given by

$$\begin{aligned}
P_{111}^{00}(m_1, m_2, m_3; \ell^2) &= \frac{-1}{n-3} \{ (m_1^2 + \ell^2) H_1(m_1, m_2, m_3) + H_2(m_1, m_2, m_3) \\
&\quad + m_2^2 H_1(m_2, m_1, m_3) + m_3^2 H_1(m_3, m_1, m_2) \} , \qquad (74)
\end{aligned}$$

$$\begin{aligned}
P_{111}^{10}(m_1, m_2, m_3; \ell^2) &= P_{111}^{01}(m_2, m_1, m_3; \ell^2) \\
&= \frac{-1}{n - \frac{5}{2}} \left[\frac{\ell^2}{2} P_{111}^{00}(m_1, m_2, m_3) - P_{211}^{20}(m_1, m_2, m_3) \right. \\
&\quad - m_1^2 H_2(m_1, m_2, m_3) - m_1^2 \ell^2 H_1(m_1, m_2, m_3) \\
&\quad - m_2^2 H_3(m_2, m_1, m_3) + m_3^2 H_2(m_3, m_2, m_1) \\
&\quad \left. + m_3^2 H_3(m_3, m_2, m_1) \right] , \qquad (75)
\end{aligned}$$

$$\begin{aligned}
P_{111}^{11}(m_1,m_2,m_3;\ell^2) &= \frac{-1}{n-2}\Big[m_2^2P_{211}^{11}(m_2,m_1,m_3) - m_3^2P_{211}^{11}(m_3,m_2,m_1) \\
&\quad -m_3^2P_{211}^{02}(m_3,m_2,m_1) - \ell^2 m_3^2 P_{211}^{01}(m_3,m_2,m_1) \\
&\quad +m_1^2P_{211}^{11}(m_1,m_2,m_3) - P_{211}^{21}(m_1,m_2,m_3) \\
&\quad +\frac{\ell^2}{2}P_{111}^{01}(m_1,m_2,m_3)\Big]\,, \qquad (76)
\end{aligned}$$

$$\begin{aligned}
P_{111}^{02}(m_1,m_2,m_3;\ell^2) &= P_{111}^{20}(m_2,m_1,m_3;\ell^2) \\
&= \frac{-1}{n-2}\Big[m_2^2P_{211}^{20}(m_2,m_1,m_3) + m_3^2P_{211}^{02}(m_3,m_2,m_1) \\
&\quad +m_1^2P_{211}^{02}(m_1,m_2,m_3) - P_{211}^{12}(m_1,m_2,m_3)\Big]\,. \qquad (77)
\end{aligned}$$

For the three-point functions, we use [17]

$$P_{211}^{00}(m_1,m_2,m_3;\ell^2) = H_1(m_1,m_2,m_3)\,, \qquad (78)$$

$$P_{211}^{10}(m_1,m_2,m_3;\ell^2) = -H_2(m_1,m_2,m_3) - \ell^2 H_1(m_1,m_2,m_3)\,, \qquad (79)$$

$$P_{211}^{01}(m_1,m_2,m_3;\ell^2) = -H_3(m_1,m_2,m_3)\,, \qquad (80)$$

$$\begin{aligned}
P_{211}^{20}(m_1,m_2,m_3;\ell^2) &= H_4(m_1,m_2,m_3) + \frac{\ell^2}{n}\Big\{\Big[(n-1)\ell^2 - m_1^2\Big]H_1(m_1,m_2,m_3) \\
&\quad +2(n-1)H_2(m_1,m_2,m_3) + P_{111}^{00}(m_1,m_2,m_3)\Big\}\,, \qquad (81)
\end{aligned}$$

$$\begin{aligned}
P_{211}^{11}(m_1,m_2,m_3;\ell^2) &= H_5(m_1,m_2,m_3) + \ell^2 H_3(m_1,m_2,m_3) \\
&\quad +\frac{\ell^2}{2n}\Big[(m_1^2+m_2^2-m_3^2+\ell^2)H_1(m_1,m_2,m_3) \\
&\quad +2H_2(m_1,m_2,m_3) - P_{111}^{00}(m_1,m_2,m_3) \\
&\quad +T_2(m_1^2)T_1(m_2^2) - T_2(m_1^2)T_1(m_3^2)\Big\}\,, \qquad (82)
\end{aligned}$$

$$\begin{aligned}
P_{211}^{02}(m_1,m_2,m_3;\ell^2) &= H_6(m_1,m_2,m_3) + \frac{\ell^2}{n}\Big[-m_2^2H_1(m_1,m_2,m_3) \\
&\quad +T_2(m_1^2)T_1(m_3^2)\Big]\,, \qquad (83)
\end{aligned}$$

$$\begin{aligned}
P_{211}^{30}(m_1,m_2,m_3;\ell^2) &= -H_7(m_1,m_2,m_3) - P_{111}^{10}(m_1,m_2,m_3) \\
&\quad -\frac{3\ell^2}{n+2}\Big\{\Big(\frac{n-1}{3}\ell^2 - m_1^2\Big)\ell^2 H_1(m_1,m_2,m_3) \\
&\quad +\Big[(n-1)\ell^2 - m_1^2\Big]H_2(m_1,m_2,m_3) + nH_4(m_1,m_2,m_3)\Big\}\,, \qquad (84)
\end{aligned}$$

$$P_{211}^{21}(m_1,m_2,m_3;\ell^2) = -H_8(m_1,m_2,m_3) - \frac{3\ell^2}{n+2}\Big[\frac{2}{3}(n-1)H_5(m_1,m_2,m_3)$$

$$\begin{aligned}
&+\left(\frac{n-1}{3}\ell^2 - m_1^2\right) H_3(m_1,m_2,m_3) - P^{01}_{111}(m_1,m_2,m_3)\Big] \\
&-\frac{n-1}{n(n+2)}\ell^4 \Big[(m_1^2+m_2^2-m_3^2+\ell^2)H_1(m_1,m_2,m_3) \\
&+2H_2(m_1,m_2,m_3) - P^{00}_{111}(m_1,m_2,m_3) \\
&+T_2(m_1^2)T_1(m_2^2) - T_2(m_1^2)T_1(m_3^2)\Big] \ ,
\end{aligned} \tag{85}$$

$$\begin{aligned}
P^{12}_{211}(m_1,m_2,m_3;\ell^2) \ = \ &-H_9(m_1,m_2,m_3) - \ell^2 H_6(m_1,m_2,m_3) \\
&-\frac{\ell^2}{n+2}\Big[2H_5(m_1,m_2,m_3) + \left(\frac{2\ell^2}{n} - m_2^2\right) H_2(m_1,m_2,m_3) \\
&+(m_1^2+m_2^2-m_3^2+\ell^2)H_3(m_1,m_2,m_3) \\
&+P^{01}_{111}(m_1,m_2,m_3)\Big] - \frac{\ell^4}{n(n+2)}\Big\{-P^{00}_{111}(m_1,m_2,m_3) \\
&\Big[m_1^2 - (n+1)m_2^2 - m_3^2 + \ell^2\Big] H_1(m_1,m_2,m_3) \\
&+T_2(m_1^2)T_1(m_2^2) - (n-1)T_2(m_1^2)T_1(m_3^2)\Big\} \ ,
\end{aligned} \tag{86}$$

$$\begin{aligned}
P^{03}_{211}(m_1,m_2,m_3;\ell^2) \ = \ &-H_{10}(m_1,m_2,m_3) - \frac{3\ell^2}{n+2}\Big[-m_2^2 H_3(m_1,m_2,m_3) \\
&+\ell^2 T_2(m_1^2)T_1(m_3^2)\Big] \ .
\end{aligned} \tag{87}$$

The functions of H_i are expressed as follows

$$\begin{aligned}
H_1(m_1,m_2,m_3;\ell^2) \ = \ &\pi^4\Big[\frac{2}{\Delta^2} - \frac{1}{\Delta}(1-2\gamma_{m_1}) - \frac{1}{2} + \frac{\pi^2}{12} - \gamma_{m_1} + \gamma_{m_1}^2 \\
&+h_1(m_1,m_2,m_3)\Big] \ ,
\end{aligned} \tag{88}$$

$$\begin{aligned}
H_2(m_1,m_2,m_3;\ell^2) \ = \ &\pi^4\ell^2\Big[-\frac{2}{\Delta^2} + \frac{1}{\Delta}(\frac{1}{2} - 2\gamma_{m_1}) + \frac{13}{8} - \frac{\pi^2}{12} + \frac{\gamma_{m_1}}{2} - \gamma_{m_1}^2 \\
&-h_2(m_1,m_2,m_3)\Big] \ ,
\end{aligned} \tag{89}$$

$$\begin{aligned}
H_3(m_1,m_2,m_3;\ell^2) \ = \ &\pi^4\ell^2\Big[\frac{1}{\Delta^2} - \frac{1}{\Delta}(\frac{1}{4} - \gamma_{m_1}) - \frac{13}{16} + \frac{\pi^2}{24} - \frac{\gamma_{m_1}}{4} + \frac{\gamma_{m_1}^2}{2} \\
&+ h_3(m_1,m_2,m_3)\Big] \ ,
\end{aligned} \tag{90}$$

$$\begin{aligned}
H_4(m_1,m_2,m_3;\ell^2) \ = \ &\pi^4\ell^4\Big[\frac{3}{2\Delta^2} + \frac{1}{\Delta}\frac{3\gamma_{m_1}}{2} - \frac{175}{96} + \frac{\pi^2}{16} + \frac{3\gamma_{m_1}^2}{4} \\
&+ \frac{3}{4}h_4(m_1,m_2,m_3)\Big] \ ,
\end{aligned} \tag{91}$$

$$\begin{aligned}
H_5(m_1,m_2,m_3;\ell^2) \ = \ &\pi^4\ell^4\Big[-\frac{3}{4\Delta^2} - \frac{1}{\Delta}\frac{3\gamma_{m_1}}{4} + \frac{175}{192} - \frac{\pi^2}{32} - \frac{3\gamma_{m_1}^2}{8} \\
&- \frac{3}{4}h_5(m_1,m_2,m_3)\Big] \ ,
\end{aligned} \tag{92}$$

$$H_6(m_1,m_2,m_3;\ell^2) = \pi^4\ell^4\left[\frac{1}{2\Delta^2}-\frac{1}{\Delta}(\frac{1}{24}-\frac{\gamma_{m_1}}{2})-\frac{19}{32}+\frac{\pi^2}{48}-\frac{\gamma_{m_1}}{24} + \frac{\gamma_{m_1}^2}{4}+\frac{3}{4}h_6(m_1,m_2,m_3)\right], \tag{93}$$

$$H_7(m_1,m_2,m_3;\ell^2) = \pi^4\ell^6\left[-\frac{1}{\Delta^2}-\frac{1}{\Delta}(\frac{5}{24}+\gamma_{m_1})+\frac{287}{192}-\frac{\pi^2}{24}-\frac{5\gamma_{m_1}}{24} - \frac{\gamma_{m_1}^2}{2}-\frac{1}{2}h_7(m_1,m_2,m_3)\right], \tag{94}$$

$$H_8(m_1,m_2,m_3;\ell^2) = \pi^4\ell^6\left[\frac{1}{2\Delta^2}+\frac{1}{\Delta}(\frac{5}{48}+\frac{\gamma_{m_1}}{2})-\frac{287}{384}+\frac{\pi^2}{48}+\frac{5\gamma_{m_1}}{48} + \frac{\gamma_{m_1}^2}{4}+\frac{1}{2}h_8(m_1,m_2,m_3)\right], \tag{95}$$

$$H_9(m_1,m_2,m_3;\ell^2) = \pi^4\ell^6\left[-\frac{1}{3\Delta^2}-\frac{1}{\Delta}(\frac{1}{24}+\frac{\gamma_{m_1}}{3})+\frac{95}{192}-\frac{\pi^2}{72}-\frac{\gamma_{m_1}}{24} - \frac{\gamma_{m_1}^2}{6}-\frac{1}{2}h_9(m_1,m_2,m_3)\right], \tag{96}$$

$$H_{10}(m_1,m_2,m_3;\ell^2) = \pi^4\ell^6\left[\frac{1}{4\Delta^2}+\frac{1}{\Delta}(\frac{1}{96}+\frac{\gamma_{m_1}}{4})-\frac{283}{768}+\frac{\pi^2}{96}+\frac{\gamma_{m_1}}{96} + \frac{\gamma_{m_1}^2}{8}+\frac{1}{2}h_{10}(m_1,m_2,m_3)\right], \tag{97}$$

where $\Delta = -2\epsilon$ and $\gamma_m = \gamma + \ln(\pi m^2/\mu^2)$.

The ultraviolet finite parts $h_i(m_1,m_2,m_3)$ of the function $H_i(m_1,m_2,m_3;\ell^2)$ have the following one-dimensional integral representations:

$$h_1(m_1,m_2,m_3) = \int_0^1 dy[g(y)],$$

$$h_2(m_1,m_2,m_3) = \int_0^1 dy[g(y)+f_1(y)],$$

$$h_3(m_1,m_2,m_3) = \int_0^1 dy[g(y)+f_1(y)](1-y),$$

$$h_4(m_1,m_2,m_3) = \int_0^1 dy[g(y)+f_1(y)+f_2(y)],$$

$$h_5(m_1,m_2,m_3) = \int_0^1 dy[g(y)+f_1(y)+f_2(y)](1-y),$$

$$h_6(m_1,m_2,m_3) = \int_0^1 dy[g(y)+f_1(y)+f_2(y)](1-y)^2,$$

$$h_7(m_1,m_2,m_3) = \int_0^1 dy[g(y)+f_1(y)+f_2(y)+f_3(y)],$$

$$
\begin{aligned}
h_8(m_1,m_2,m_3) &= \int_0^1 dy[g(y)+f_1(y)+f_2(y)+f_3(y)](1-y)\,, \\
h_9(m_1,m_2,m_3) &= \int_0^1 dy[g(y)+f_1(y)+f_2(y)+f_3(y)](1-y)^2\,, \\
h_{10}(m_1,m_2,m_3) &= \int_0^1 dy[g(y)+f_1(y)+f_2(y)+f_3(y)](1-y)^3\,. \qquad (98)
\end{aligned}
$$

All ten integral representations are built up by the following four basic functions:

$$
\begin{aligned}
g(y) &= Sp\left(\frac{1}{1-y_1}\right)+Sp\left(\frac{1}{1-y_2}\right)+y_1\ln\left(\frac{y_1}{y_1-1}\right)+y_2\ln\left(\frac{y_2}{y_2-1}\right)\,, \\
f_1(y) &= \frac{1}{2}\left[-\frac{1-\nu^2}{\kappa^2}+y_1^2\ln\left(\frac{y_1}{y_1-1}\right)+y_2^2\ln\left(\frac{y_2}{y_2-1}\right)\right]\,, \\
f_2(y) &= \frac{1}{3}\left[-\frac{2}{\kappa^2}-\frac{1-\nu^2}{2\kappa^2}-\left(\frac{1-\nu^2}{\kappa^2}\right)^2+y_1^3\ln\left(\frac{y_1}{y_1-1}\right)+y_2^3\ln\left(\frac{y_2}{y_2-1}\right)\right]\,, \\
f_3(y) &= \frac{1}{4}\left[-\frac{4}{\kappa^2}-\left(\frac{1}{3}+\frac{3}{\kappa^2}\right)\frac{1-\nu^2}{2\kappa^2}-\frac{1}{2}\left(\frac{1-\nu^2}{\kappa^2}\right)^2-\left(\frac{1-\nu^2}{\kappa^2}\right)^3\right. \\
&\qquad \left.+y_1^4\ln\left(\frac{y_1}{y_1-1}\right)+y_2^4\ln\left(\frac{y_2}{y_2-1}\right)\right]\,, \qquad (99)
\end{aligned}
$$

where

$$
\begin{aligned}
Sp(z) &= \int_0^z -\frac{\ln(1-t)}{t}dt\,, \\
y_{1,2} &= \frac{1+\kappa^2-\nu^2\pm\sqrt{(1+\kappa^2-\nu^2)^2+4\nu^2\kappa^2-4i\kappa^2\eta}}{2\kappa^2}\,, \\
\nu^2 &= \frac{ay+b(1-y)}{y(1-y)}\,,\quad a=\frac{m_2^2}{m_1^2}\,,\quad b=\frac{m_3^2}{m_1^2}\,,\quad \kappa^2=\frac{\ell^2}{m_1^2}\,. \qquad (100)
\end{aligned}
$$

Finally, we must transform the parameters back into the Minkowski space and change the inward directions of the momenta l,k for the final particles by outward ones:

$$
\begin{aligned}
\ell^2 &\to -(m_{K,\pi}^2-2p\cdot k)\,, \\
\ell'^2 &\to -[m_{K,\pi}^2-2p\cdot k(1-x)]\,, \\
p\cdot k &\to p\cdot k\,, \\
p\cdot\ell' &\to m_{K,\pi}^2-p\cdot k(1-x)\,, \\
k\cdot\ell' &\to -p\cdot k\,, \qquad (101)
\end{aligned}
$$

where $0 \leq p \cdot k \leq (m_{K,\pi}^2 - m_\ell^2)/2$, and we have replaced ∂^2 by $-\partial^2$ as calculated in the Euclidian space.

References

[1] J. Gasser and H. Leutwyler, Ann. Phys. 158 (1984) 142.

[2] J. Gasser and H. Leutwyler, Nucl. Phys. B250 (1985) 465.

[3] A. Pich, Rep. Prog. Phys. 58 (1995) 563.

[4] V. Bernard, N. Kaiser and Ulf-G. Meissner, J. Mod. Phys. E4 (1995) 193.

[5] G. Ecker, Prog. Part. Nucl. Phys. 35 (1995) 1.

[6] J. Bijnens, G. Ecker and J. Gasser, "Chiral perturbation theory" [arXiv:hep-ph/9411232]; J. Bijnens, G. Colangelo, G. Ecker and J. Gasser, "Semileptonic kaon decays" [arXiv:hep-ph/9411311]; in "The Second Daphne Physics Handbook", eds. L. Maiani, G. Pancheri and N. Paver, INFN-Frascati, 1995.

[7] J. Bijnens, G. Ecker and J. Gasser, Nucl. Phys. B **396** 81 (1993) 81 [arXiv:hep-ph/9209261].

[8] V. N. Bolotov, Phys. Lett. B243 (1990) 308.

[9] A. A. Poblaguev, Phys. Lett. B238 (1990) 109.

[10] S. C. Adler *et al.* [E787 Collaboration], Phys. Rev. Lett. **85**, 2256 (2000) [arXiv:hep-ex/0003019].

[11] V. V. Anisimovsky *et al.* [KEK E246 Collaboration], arXiv:hep-ex/0304027.

[12] C. Q. Geng and S. K. Lee, Phys. Rev. D **51**, 99 (1995) [arXiv:hep-ph/9410347].

[13] C. H. Chen, C. Q. Geng and C. C. Lih, Phys. Rev. D **56** (1997) 6856 [arXiv:hep-ph/9709447].

[14] J. Bijnens, G. Colangelo and G. Ecker, JHEP 9902 (1999) 020 [hep-ph/9902437].

[15] H. W. Fearing and S. Scherer, Phys. Rev. D53 (1996) 315.

[16] T. Ebertshauser, H. W. Fearing, and S. Scherer, Phys. Rev. D65 (2002) 054033 [hep-ph/0110261].

[17] A. Ghinculov and York-Peng Yao, Nucl. Phys B516 (1998) 385 [hep-ph/9702266].

[18] P. Post and J. B. Tausk, Mod. Phys. Lett. A11 (1996) 2115.

[19] T. N. Truong, Phys. Rev. Lett. 61 (1988) 2526.

[20] A. Dobado, M. J. Herrero and T. N. Truong, Phys. Lett. B235 (1990) 134.

[21] T. N. Truong, EFI-90-26-CHICAGO *Lectures given at Ettore Majoranava International School on Low Energy Antiproton Physics, Erice, Italy, Jan 25-31, 1990.*

[22] J. Bijnens, G. Colangelo and G Ecker, JHEP 9902 (1999) 020; Ann. Phys. B280 (2000) 100 [hep-ph/9907333].

[23] L. Ametller, J. Bijnens, A. Bramon and F. Cornet, Phys. Lett. B303 (1993) 140 [hep-ph/9302219].

[24] J. Bijnens and P. Talavera, Nucl. Phys. B489 (1997) 387 [hep-ph/9610269].

[25] M. Knecht and A. Nyffeler, Eur. Phys. J. C21 (2001) 659 [hep-ph/0106034].

[26] John F. Donoghue and Barry R. Holstein, phys Rev. D40 (1989) 2378.

[27] John F. Donoghue and Barry R. Holsetin, phys. Rev. D40 (1989) 3700

[28] P. Post and K. Schilcher, Eur. Phys. J. C25 (2002) 427 [hep-ph/0112352].

[29] Olof Strandberg, hep-ph/0302064.

[30] J. Bijnens, A. Bramon and F. Cornet, Phys. Rev. Lett. 61 (1988) 1453.

[31] J. Bijnens, A. Bramon and F. Cornet, Phys. Lett. B237 (1990) 488

[32] J. Bijnens, Private Communication.

[33] G. Amoros, J. Bijnens and P. Talavera, Nucl. Phys. B **602** (2001) 87 [arXiv:hep-ph/0101127].

[34] J. Bijnens and P. Talavera, arXiv:hep-ph/0303103; J. Bijnens and P. Talavera, JHEP **0203** (2002) 046 [arXiv:hep-ph/0203049]; G. Amoros, J. Bijnens and P. Talavera, Nucl. Phys. B **585** (2000) 293 [Erratum-ibid. B **598** (2001) 665] [arXiv:hep-ph/0003258]; G. Amoros, J. Bijnens and P. Talavera, Nucl. Phys. B **568** (2000) 319 [arXiv:hep-ph/9907264]; E. Golowich and J. Kambor, Nucl. Phys. B **447**, 373 (1995) [arXiv:hep-ph/9501318]; E. Golowich and J. Kambor, Phys. Rev. D **58**, 036004 (1998) [arXiv:hep-ph/9710214].

[35] S. Scherer, arXiv:hep-ph/0210398.

[36] J. Prades, Z. Phys. C63 (1994) 491; Erratum: Eur. Phys. J. C11 (1999) 571.

[37] A. A. Poblaguev *et al.*, Phys. Rev. Lett. **89** (2002) 061803 [arXiv:hep-ex/0204006].

[38] F. L. Bezrukov, D. S. Gorbunov and Y. G. Kudenko, Phys. Rev. D **67** (2003) 091503 [arXiv:hep-ph/0302106].

[39] Particle Data Group, K. Hagiwara *et al.*, Phys. Rev. D66 (2002) 010001.

[40] C. Q. Geng, C. C. Lih and W. M. Zhang, Phys. Rev. D **57** (1998) 5697 [arXiv:hep-ph/9710323].

[41] C. Q. Geng, C. C. Lih and C. C. Liu, Phys. Rev. D **62** (2000) 034019 [arXiv:hep-ph/0004164].